

University of Kentucky

UKnowledge

---

Theses and Dissertations--Electrical and  
Computer Engineering

Electrical and Computer Engineering

---


2021

## Fabrication and Simulation of Perovskite Solar Cells

Maniell Workman

*University of Kentucky*, mwo265@uky.edu

Author ORCID Identifier:

 <https://orcid.org/0000-0002-9599-1673>

Digital Object Identifier: <https://doi.org/10.13023/etd.2021.160>

[Right click to open a feedback form in a new tab to let us know how this document benefits you.](#)

### Recommended Citation

Workman, Maniell, "Fabrication and Simulation of Perovskite Solar Cells" (2021). *Theses and Dissertations--Electrical and Computer Engineering*. 165.

[https://uknowledge.uky.edu/ece\\_etds/165](https://uknowledge.uky.edu/ece_etds/165)

This Master's Thesis is brought to you for free and open access by the Electrical and Computer Engineering at UKnowledge. It has been accepted for inclusion in Theses and Dissertations--Electrical and Computer Engineering by an authorized administrator of UKnowledge. For more information, please contact [UKnowledge@lsv.uky.edu](mailto:UKnowledge@lsv.uky.edu).

## **STUDENT AGREEMENT:**

I represent that my thesis or dissertation and abstract are my original work. Proper attribution has been given to all outside sources. I understand that I am solely responsible for obtaining any needed copyright permissions. I have obtained needed written permission statement(s) from the owner(s) of each third-party copyrighted matter to be included in my work, allowing electronic distribution (if such use is not permitted by the fair use doctrine) which will be submitted to UKnowledge as Additional File.

I hereby grant to The University of Kentucky and its agents the irrevocable, non-exclusive, and royalty-free license to archive and make accessible my work in whole or in part in all forms of media, now or hereafter known. I agree that the document mentioned above may be made available immediately for worldwide access unless an embargo applies.

I retain all other ownership rights to the copyright of my work. I also retain the right to use in future works (such as articles or books) all or part of my work. I understand that I am free to register the copyright to my work.

## **REVIEW, APPROVAL AND ACCEPTANCE**

The document mentioned above has been reviewed and accepted by the student's advisor, on behalf of the advisory committee, and by the Director of Graduate Studies (DGS), on behalf of the program; we verify that this is the final, approved version of the student's thesis including all changes required by the advisory committee. The undersigned agree to abide by the statements above.

Maniell Workman, Student

Dr. Zhi David Chen, Major Professor

Dr. Daniel L. Lau, Director of Graduate Studies

FABRICATION AND SIMULATION OF PEROVSKITE SOLAR CELLS

---

THESIS

---

A thesis submitted in partial  
fulfillment for the degree of Master of Science in  
Electrical Engineering in the College of Engineering  
at the University of Kentucky

By

Maniell Elijah Workman

Lexington, Kentucky

Director: Dr. Zhi David Chen, Professor of Electrical Engineering

Lexington, Kentucky

2021

Copyright © Maniell Workman 2021  
<https://orcid.org/0000-0002-9599-1673>

## ABSTRACT OF THESIS

### Fabrication and Simulation of Perovskite Solar Cells

Since the dawning of the industrial revolution, the world has had a need for mass energy production. In the 1950s silicon solar panels were invented. Silicon solar panels have been the main source of solar energy production. They have set the standard for power conversion efficiency for subsequent generations of photovoltaic technology. Solar panels utilize light's ability to generate an electron hole pair. By creating a PN Junction in the photovoltaic semiconductor, the electron and hole are directed in opposing layers of the solar panel generating the electric current. Second generation solar panels utilized different thin film materials to fabricate solar panels. Materials such as Cadmium Telluride, Copper Indium Gallium Selenide, and amorphous silicon. This technology is now seen commercially available around the world. In the research community a third generation of solar panel technology is being developed. Perovskites are an emerging third generation solar panel technology. Perovskites' power conversion efficiency have increased from 3.8% to 24.2% over the span of a decade. Perovskite crystals have desirable optical properties such as a high absorption coefficient, long carrier diffusion length, and high photoluminescence. The most prominent types of perovskites for solar cell research are organic metal halide perovskites. These perovskites utilize the desirable properties of organic electronics. Electrochemical techniques such as additives, catalysts, excess of particular chemicals, and variations in antisolvents impact the electronic properties of the perovskite crystal. The perovskite is however on layer of the device. Solar cell devices incorporate multiple layers. The materials for the electron transport layer, hole transport material, and choice of metal electrode have an impact on device performance and the current voltage relationship. Current silicon photovoltaic devices are more expensive than conventional fossil fuel. Modeling perovskite solar cells in a simulated environment is critical for data analytics, real fabrication behavior projection, and quantum mechanics of the semiconductor device. Photovoltaic semiconductors are diodes which produce a current when exposed to light. The ideality factor is a parameter which tells how closely a semiconductor behaves to an ideal diode. In an ideal diode, the only mechanism for hole electron recombination is direct bimolecular recombination. Because there are multiple mechanisms of recombination, there are no real devices with a perfect ideality factor. The types of recombination occurring within a device can be inferred by its ideality factor. In this research. Analyzing fabricated perovskite solar cells using their ideality factor can indicate which type of recombination is dominant in the device. The interaction between the perovskite crystal and transport layers is of high interest as differentials in energy level bands can hinder overall power conversion efficiency and act as a site for nonradiative recombination loss. In addition, the use of Machine Learning (ML) to research and predict the opto-electronic properties of perovskite can greatly accelerate the development of this technology. ML techniques such as Linear Regression (LR), Support Vector Regression (SVR), and Artificial Neural Networks (ANNs) can greatly improve the chemical processing and manufacturing techniques. Such tools used to improve this technology have major impacts for the further proliferation of solar energy on a national scale. These tools

can also be used to optimize power conversion efficiency of perovskites, This optimization is critical for commercial use of perovskite solar panel technology. Various electrochemical and fabrication strategies are currently being researched in order to optimize power conversion efficiency and minimize energy loss. There are current results which suggest the addition of particular ions in the perovskite crystal have a positive impact on the power conversion efficiency. The qualities of the cell such as crystallinity, defects, and grain size play important roles in the electrical properties of the cell. Along with the quality of the perovskite crystal, its interfacing with the transport layers plays a critical role in the operation of the device. In this thesis, perovskite solar cells are fabricated and simulated to research their optoelectronic properties. The optoelectronic behavior of simulated solar cells is manipulated to match that of cells. By researching this new optoelectronic material in a virtual environment, applicability and plausibility are demonstrated. This legitimizes the continued research of this third-generation solar panel material.

KEYWORDS: Perovskite, open circuit voltage, short circuit current, fill factor, morphology, power conversion efficiency

---

Maniell Elijah Workman

*(Name of Student)*

---

04/30/2021

Date

Fabrication and Simulation of Perovskite Solar Cells

By  
Maniell Elijah Workman

Dr. David Zhi Chen

---

Director of Thesis

Dr. Daniel L. Lau

---

Director of Graduate Studies

04/30/2021

---

Date

## DEDICATION

*To my beloved late brother Iroquois Tyrese Alston. Your love and brilliance transcend your death. Your life and your pain taught me that even amid the cruelties that life is capable of love can still exist. The pain that is your physical absence may not heal but the love you left can help. Of the over 14,000 killed in 2011, I could have never imagined your name would be on that list. Your story is one of thousands of young, talented, promising black men taken by what some call the streets. Streets which look upon me in anticipation of my demise. Your plight is mine. The plight of being a displaced African on a continent called America running from their death. With every step I take bated breaths. Knowing at any time and at any place my name could join the list in a graveyard. With every lesson I learn I think of your brilliance. Had your dream not been differed, you could have joined me in academia and greatness. It is for you my brother Iroquois Alston, and for all my brothers taken too soon that I do this. I fight to be a little bit better, stronger, and smarter for all my brothers taken too soon.*

## ACKNOWLEDGMENTS

While this research was an individual effort it is with great pleasure I acknowledge my advisor Dr. Zhi David Chen. With your guidance and support of my graduate studies I have achieved a major goal in my life.

I would also like to extend my sincere acknowledgments in gratitude to Dr. Sarhan Musa. Our publications on perovskite solar cell research were a tremendous contribution to me as a graduate student and as a researcher. The value of our work for my graduation and my technical writing cannot be measured. It is with the utmost high sincerity that I thank Dr. Sarhan Musa for collaborating with me and mentoring me.

I would like to thank my committee member and colleague Dr. Jeffery Hastings. Your insightful lessons and inputs into my development as a graduate student has been greatly appreciated. I would also like to acknowledge Dr. Kenneth Graham. The access granted to your lab equipment was critical to achieving the results required for this thesis. I would also like to acknowledge my former lab mates Dr. Hojjatollah Sarvari and Guoduan Liu. I would also like to acknowledge Dr. Somin Park for her help in my research efforts.



## TABLE OF CONTENTS

<b>Fabrication and Simulation of Perovskite Solar Cells .....</b>	<b>i</b>
<b>ABSTRACT OF THESIS.....</b>	<b>i</b>
<b>ACKNOWLEDGMENTS .....</b>	<b>iii</b>
<b>LIST OF TABLES .....</b>	<b>v</b>
<b>LIST OF FIGURES .....</b>	<b>vi</b>
<b>CHAPTER 1. introduction .....</b>	<b>8</b>
1.1 Physics of Semiconductors.....	8
1.1 Optoelectronics .....	9
1.2 Solar Energy.....	11
1.2.1 Thin Film Solar Panels.....	13
1.2.2 Power Engineering .....	15
1.2.3 Power Quality.....	16
1.2.4 Smart Grid Technology .....	17
Perovskite Optoelectronics .....	22
1.2.5 Optical and Electrical Properties .....	22
1.2.6 Electrochemistry.....	23
1.2.7 Perovskite Solar Cells.....	24
Simulation and Modeling.....	29
1.2.8 Machine Learning .....	30
1.2.9 Data Analytics.....	35
<b>CHAPTER 2. Background of perovskite research.....</b>	<b>39</b>
Electron Transport Layer.....	39
Perovskite Optical Absorption Layer.....	41
Hole Transport Layer .....	44
<b>CHAPTER 3. methodology.....</b>	<b>47</b>
Semiconductor Fabrication .....	47
Substrate Cleaning .....	48
Tin (IV) Oxide Deposition .....	51
Perovskite Crystal Fabrication .....	53
Hole Transport Layer .....	54
Gold Electrodes.....	56

<i>Results and Discussion</i> .....	58
<b>CHAPTER 4. Data collection methodology</b> .....	<b>61</b>
4.1 <i>Data Acquisition and Analysis</i> .....	61
4.2 <i>Fabricated Sample Testing</i> .....	61
<b>CHAPTER 5. Simulation of Perovskite solar cells</b> .....	<b>67</b>
5.1 <i>Perovskite Solar Cell Simulation</i> .....	67
<b>CHAPTER 6. conclusion and future work</b> .....	<b>75</b>
6.1 <i>Conclusion</i> .....	75
6.2 <i>Future Work</i> .....	76
<b>BIBLIOGRAPHY</b> .....	<b>79</b>
<b>maniell workman vita</b> .....	<b>84</b>

## LIST OF TABLES

Table 1.1 Perovskite precursor solution materials and weights.....	53
Table 2.1 HTM materials and weights.....	55
Table 3.1 Simulation of a Solar Module with PSK and Commercial Solar Module .....	72

## LIST OF FIGURES

Figure 1: Layers of a typical solar panel [5].	13
Figure 2: Typical configuration of CdTe/CdS solar cell [8].	15
Figure 3: Breakdown by source of energy production in 2020 [10].	16
Figure 4: Perovskite crystal structure [15].	22
Figure 5: Power Conversion Efficiencies of various researched materials [16].	23
Figure 6: The power conversion efficiency of solar cells with titanium oxide and tin oxide over one thousand hours [22].	27
Figure 7: The layers of the fabricated device. The bottom layer, deposited first, is the electron transport layer comprised of Tin (IV) Oxide nanoparticles, Perovskite crystal of $\text{Cs}_{0.05}(\text{MA}_{0.17}\text{FA}_{0.83})_{0.95}\text{Pb}(\text{I}_{0.83}\text{Br}_{0.17})_3$ , Organic Hole transport layer, top electrode of gold. .	48
Figure 8: Multimeter reading of glass surface.	49
Figure 9 1: Water cleaning station.	50
Figure 10: UV Ozone cleaner required.	52
Figure 11 1: Resistance of quality electron transport layer of Tin (IV) Oxide nanoparticles on FTO.	53
Figure 12 1: Correct removal of films for gold deposition.	56

Figure 13 1: The fabricated perovskite solar cells after gold deposition. ....	58
Figure 14 1: Current voltage relationship of Perovskite solar cell. ....	59
Figure 15 1: Current voltage relationship of Perovskite solar cell. ....	59
Figure 16 1: Current voltage relationship of Perovskite solar cell. ....	60
Figure 17 1: Current voltage relationship of Perovskite solar cell. ....	60
Figure 18 1: Solar Simulator Setup with multimeter. ....	62
Figure 19 1: Back Power switch of Solar Simulator.....	63
Figure 19 2: Front Power switch of Solar Simulator. ....	63
Figure 20 1: KaleidaGraph screen after data is populated.....	66
Figure 21 1: Current voltage curve of fabricated cell and simulated PSC.....	67
Figure 22 1: Current voltage relationship of fabricated perovskite cell. ....	70
Figure 23 1: Current voltage relationship of fabricated perovskite cell. ....	70
Figure 24 1: PSC with 2 nm of silver deposited and its corresponding simulated cell. ...	71
Figure 25 1: Layer construction of PSC with 2 nm Silver layer.....	71

## CHAPTER 1. INTRODUCTION

### 1.1 Physics of Semiconductors

In electronics, the two main categories of electronics were conductors and insulators. Conductors which allow a high amount of electrical current in response to a voltage. These are typically metals or materials which have a high electric field permeability. Insulators are materials which do not produce a current in response to a voltage. Semiconductors have been the subject of research since the 19<sup>th</sup> century. In 1954, the first Silicon transistor was made [1]. Semiconductors are materials which conduct electricity under particular circumstances. Semiconductor materials have been used to fabricate numerous types of electronic devices such as diodes, transistors, and optoelectronics. Diodes are semiconductors which allow current to flow in one direction above a certain voltage. Diodes are typically made with silicon or germanium. Diodes are made by doping a semiconductor material with different elements to create a PN Junction. A PN junction is an intrinsic electric field created by doping a semiconductor crystal with an element with more free electrons in one portion and a less free electrons in the opposing region. The diffusion of electrons from the region with high electron concentrations (the N region) and low concentration (P region) creates an internal electric field [2]. This intrinsic field creates the necessary voltage level required for electric current to flow. This configuration is called forward bias. When a voltage which is negative is applied to the diode, the configuration is called reverse bias. In reverse bias the electric field increases in size and forbids electric current. Since the creation of the diode, numerous different types

of diodes and transistors have been created. Each type of diode and transistor has unique properties.

Transistors are a class of diodes with multiple inputs and junctions. The first point contact transistor was invented in bell labs in 1947 [3]. Transistors are semiconductor devices whose relationship with current and voltage can be described by a mathematical equation. These nonlinear devices can be used as switches, rectifiers, and memory for computers. Field Effect Transistors are semiconductors which use the voltage applied at one gate to generate current between two other electrodes. Field effect transistors (FET) have many subdivisions. Metal Oxide FETs (MOSFET) are transistors with a metal oxide at one gate as an impeding layer. This passivation made the transistor more reliable by controlling the current through a capacitive gate. Bipolar junction transistors (BJT) use both electrons and holes to produce current. These transistors can be used as amplifiers for current and voltage, and as switches. By using the quantum mechanics of the PN junction and well understood electrical concepts, Semiconductors have revolutionized Electrical Engineering and computing. This impact of semiconductors is difficult to overstate.

### 1.1 Optoelectronics

In quantum mechanics, photons or quantified wave packets of light has been shown to have interesting interactions with matter. Light is a propagating electromagnetic wave which has momentum but not mass. The photoelectric effect is the ability for light to free an electron from its host atom. While all materials are subject to this phenomenon, some materials exhibit far more activity under illumination then others. The field of optoelectronics has exploited this phenomenon to create electronic devices with predictable behaviors in response to illumination. This field has created a slew of opto

electronic devices such as phototransistors, Light Emitting Diodes (LED), solar panels, and lasers. In the fields of optoelectronics, there are many critical parameters and factors which determine the devices operations. Currently engineers can manipulate these parameters to a predetermined end.

While there are many parameters which can positively and negatively influence an optoelectronic device, one of the most fundamental characteristics is its bandgap energy. The bandgap energy is the energy required to excite an electron from the highest energy level of the valence band to the lowest energy level of the conduction band. The bandgap, which is typically displayed on an energy band diagram, can tell much about the material properties. On an energy band diagram energy is plotted versus momentum. Because photons have relatively low momentum with respect to electrons the amount of momentum a photon contributes to an electron is inconsequential. Bandgap diagrams can detail information such as how efficiently electrons absorb lights, the effective mass of the electron, and how efficiently the material convert optical energy into electrical energy. A materials' bandgap typically falls into one of two categories, direct bandgap materials and indirect bandgap materials. Direct bandgap materials have the valence band maximum at the same momentum value as the conduction band minimum. These materials are highly efficient at absorbing optical energy and converting it into electrical energy and vice versa. Indirect bandgap materials have the conduction band minimum and the valence band maximum at different values of momentum. These materials we also require not only optical energy but thermal energy in the form of a phonon in order to excite an electron from the valence band to the conduction band. When an electron absorbs a photon to reach an excited state it is called Absorption. When an electron goes to a lower state and releases



a photon this process is called Emission. From these two processes, the field of optoelectronics has created in array of materials and devices.

## 1.2 Solar Energy

Bell labs first created the Silicon solar panel in the 1950s [4]. The power conversion efficiency of this first generation of Silicon solar panels was only 6%. Today's solar panels typically have power conversion efficiencies of roughly 20% commercially available. Silicon solar panels are photovoltaic devices fabricated utilizing many layers to produce electrical power. The Silicon layer acts as the optical absorption layer producing electron hole pairs which create the current. The Silicon photoactive layer is typically amorphous Silicon, polycrystalline Silicon, or monocrystalline Silicon. Amorphous Silicon solar panels are solar panels whose Silicon photoactive layer are vapor deposited on to a substrate. Polycrystalline Silicon is a solar panel whose photoactive layer is not comprised of a single crystal of Silicon. Mono crystalline Silicon is one homogeneous crystal as its optical absorption layer. This first generation of solar panel technology has become the entry standard for the subsequent generations of photovoltaic technology. Equation 1 describes the voltage current relationship of this device. This technology utilizes not only the optoelectronic properties of Silicon crystal but numerous layers in order to make solar energy possible.

$$I = I_{SC} - I_0 \left[ e^{\frac{qV}{kTn}} - 1 \right] \dots \dots \dots (1)$$

The power conversion efficiency of a solar panel given by equation 2 is how efficiently a solar panel converts optical energy into electrical energy.

$$PCE = \frac{P_{elec}}{P_{opt}} \dots\dots\dots(2)$$

Another critical parameter for solar panels to maximize is the fill factor. In the current voltage relationship of a solar cell, there is a point in which the cell delivers its maximum power. The ratio between the power delivered at this point and the product between open circuit voltage in short circuit current is called the fill factor. This fill factor is given by equation 3.

$$FF = \frac{|I_M * V_M|}{I_{SC} * V_{OC}} \dots\dots\dots(3)$$

Using the maximum power point of the current voltage relationship, the Current ( $I_M$ ) and Voltage ( $V_M$ ) at that point is compared to the short circuit current and the open circuit voltage.

A typical solar panel is a photovoltaic device which incorporates the electrical properties of numerous different layers. The back metal electrode is a metal which conducts electricity from the solar cell to the rest of the solar panel. The optical absorption layer consists of the Silicon crystal containing the PN junction which separates holes in electron pairs. A top metal grate acts as a front contact to complete the circuit. Many solar panels incorporate an antireflective coating between the front metal contact and the Silicon substrates. This acts to maximize the number of photons the Silicon crystal absorbs. This in turn maximizes the potential for the solar panels to generate electricity. This configuration can be seen in Figure 1.

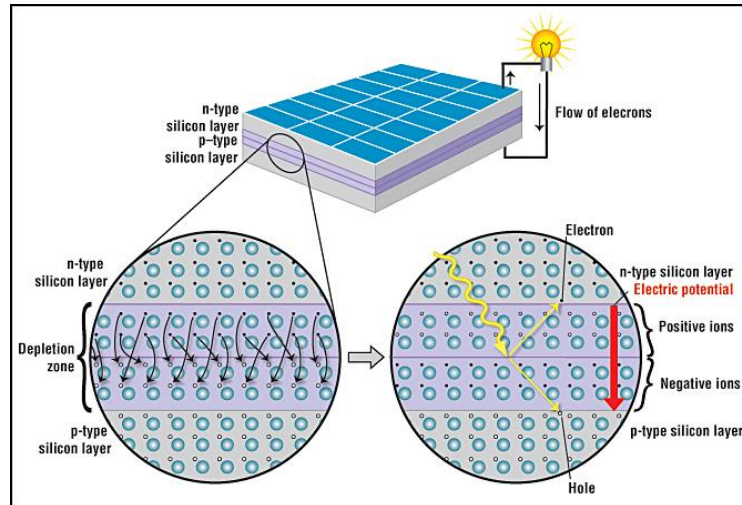


Figure 1: Layers of a typical solar panel [5].

### 1.2.1 Thin Film Solar Panels

While the role Silicon solar panels are key to the proliferation of solar energy, this technology has flaws and shortcomings. These shortcomings were the driving factor to produce a second generation of photovoltaic technology. Second generation solar panel technology can be described as thin film optoelectronic materials. This technology is a commercially available alternative to first generation solar panels. Materials such as Cadmium Telluride, Amorphous Silicon, and Copper Indium Gallium Selenide (CIGS) has good performance in commercially available solar panels. Their power conversion efficiencies have shown to be comparable to first generation Silicon solar panels. One of the main issues that thin film solar panel technology addresses is the high cost of first generation solar panels. Traditional solar panels of crystal Silicon have a very high cost of fabrication and installation. This causes the payback time of these solar panels to be quite

lengthy. Thin film solar panel technology lowers the initial cost of solar panel fabrication installation thereby shortening the payback time.

Amorphous silicon is fabricated by vapor depositing Silicon onto a substrate. Amorphous Silicon typically has a bandgap of 1.8 eV. This wide bandgap presents the possibility of using crystal in an amorphous Silicon in tandem on a solar cell [6]. This technology has also yielded microcrystalline Silicon solar panels. Second generation amorphous Silicon has quickly gained a significant sector of the solar energy market. Both amorphous and microcrystalline solar panels have been fabricated in tandem with each other in order to raise power conversion efficiency. This tandem use of these two different types of silicon structures has ameliorated the flaws seen in both types of Silicon. Amorphous Silicon solar panels have mainly been criticized because of their low power conversion efficiency and degradation time. Microcrystalline Silicon solar panels have garnered criticism due to their low current density and low open circuit voltage. Other techniques of enhancing the optoelectronic properties of an amorphous Silicon solar panel is the introduction of hydrogen. Hydrogenated amorphous Silicon has been shown to have higher short circuit current density in higher open circuit voltage. This form of amorphous Silicon has also been shown to have a higher fill factor than amorphous and amorphous microcrystalline Silicon. This second generation of silicon photovoltaic technology has shown that manipulating the material properties of the photoactive layer can have positive effects on the electric performance of the whole device.

Cadmium has played a critical role in many second generation photovoltaic devices. Unlike its predecessors, cadmium solar panels create a PN junction with the combination of two different materials. A typical cadmium based solar panel is made from

Cadmium Telluride and Cadmium Sulfide as seen in Figure 2. The Cadmium Telluride layer acts as the P type layer of the photoactive layer. As with other thin film solar devices, CdTe/CdS solar panels can be easily made through vacuum and nonvacuum manufacturing processes. CdTe/CdS solar panels have a registered power conversion efficiency of 16.7% by the National Renewable Energy Laboratory [7].

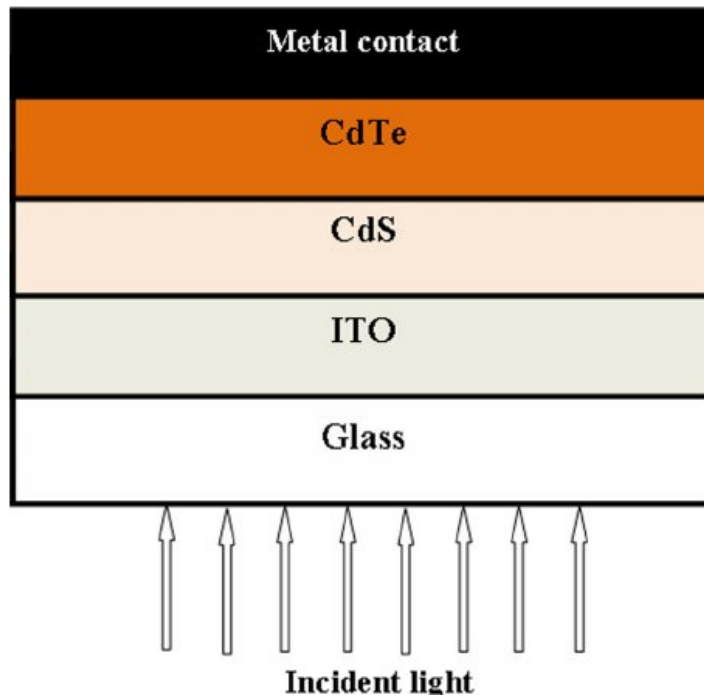


Figure 2: Typical configuration of CdTe/CdS solar cell [8].

### 1.2.2 Power Engineering

As stated by the National Academy of engineering, the electrification of the United states has been the most significant advanced in engineering in the 20th century [9]. The national power grid has been a cornerstone of our modern society for decades. The infrastructure, principles, and maintenance of this grid is the backbone of power engineering. Since the 1930s, the efficient generation and transmission of electrical power in the power grid has been the subject of many engineers' research and careers. Fossil fuels

from petroleum and oil are currently predominant method of power generation in the United States. In recent years the flaws and shortcomings of fossil fuels have become more apparent. The extraneous gases produced by the burning, refining, and utilization of fossil fuels has created the climate change crisis. Therefore, the use of environmentally friendly resources for power generation has become necessitated. Renewable energy encompasses many technologies for environmentally conscious energy production. Energy production methods such as wind turbine generation, geothermal energy, and solar energy have led the proliferation of sustainable energy production. This is just one of many issues including power quality, fault isolation, and fault correction that power engineering seeks to address.

### U.S. primary energy consumption by energy source, 2019

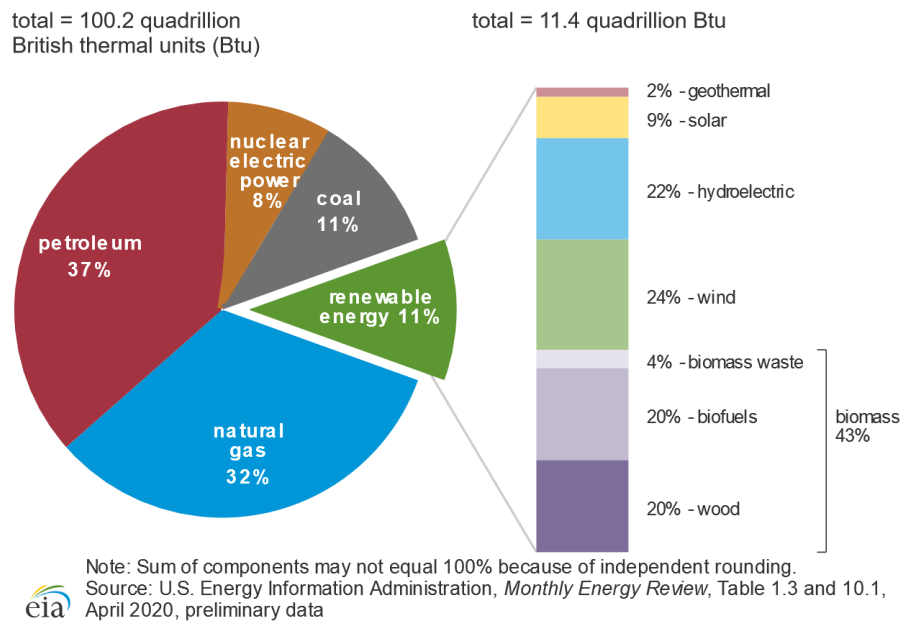


Figure 3: Breakdown by source of energy production in 2020 [10].

### 1.2.3 Power Quality

As with all advancements, standardization is required to ensure high quality product. Power quality is a critical issue in power engineering. The quality of electrical power delivered to commercial and residential customers is critical to their operation.

Drastic fluctuations in the quality of power can cost consumers large sums of money. This lead the international electrical electronics engineers (IEEE) to create power quality standards [8]. As regulated by the IEEE, total harmonic distortion must not exceed 2% for voltage and must not exceed 5% for current [11]. Harmonic distortion is the generation of higher order resonant frequencies created in the generation of Alternating Current (AC) power. Typically, power quality problems can be described as short or long interruptions. Fault isolation and analysis is the subject of ongoing research. The topology and size of the grid influences the type and frequency of power quality faults. Harmonic disturbances have posed a significant issue for microgrids with distributed energy sources. Other power quality faults such as dips and swells also pose significant risk. Swells and power can cause short circuits and failures in transmission devices. Dips can cause intermittent power failures such as brownouts and blackouts. Ensuring power quality is critical to both the safety and security of both supplier and customer.

#### 1.2.4 Smart Grid Technology

The need for energy has never seen such an all time high such as today. Reliable power is critical to the functioning of an interconnected world. The national power grid has had this aim since its creation. The infrastructure of the national power grid is becoming more obsolete as increases and changes in demand of power occur. Issues such as spikes in demand, pollution from traditional energy production, and depleting fossil fuels is necessitating new methods of energy production and transmission. The Department of Energy's proposal for a smart grid will be more economical, efficient, and environmentally conscious [12]. The theorized smart grid would have many aspects to ensure satisfactory

performance. Quality control, metering, fault detection and isolation, energy management, and communication are the subject of many research labs and commercial agencies. Fault analysis is critical the functioning of a smart grid. Faults in the power grid can have devastating costs such as total loss of power. Sensing and measurement of the grid can provide continuous or semicontinuous readings of the power and any deviations from design specifications. The fundamental design premise of the smart grid is the combination of a communication network inclusive of germane protocols with self-correcting power transmission devices.

Obsolete infrastructure is not able to handle the loads projected for the future. To handle this future load, engineers have proposed creating a smart grid for consumer's power needs. The proposed smart grid would be more reliable for delivering quality power when and where customers need it. Cybersecurity would enable the smart grid to withstand possible attacks from both foreign and domestic terrorists targeting the nation's infrastructure. The Department of Energy's proposal for a smart grid will be more economical, efficient, and environmentally conscious [13]. With the development of a national smart grid, modern power needs can be met for a technologically advanced society.

The smart grid's critical advantage is its superior measures of power quality control. Power quality control is important for both residential and commercial applications. Laboratories with highly sensitive equipment and experiments rely on constant and stable power to operate. The proposed smart grid uses distributed sensors and self-correcting infrastructure to create a self-healing grid which can react in real time to fluctuations in



power. These control measures combine the advantages of a communication network, and advanced devices.

Smart grid design utilizing a distributed microgrid structure has been shown to have many positive aspects. A microgrid is a local power grid with a means of power generation and local transmission. Microgrids can operate in island or grid connected mode. In Island mode, the microgrid can implement fault isolation and correction with an array of digital relays and communication overlay. In grid connected mode, the generators must be synchronized and corrected with grid feeding control. This will ensure that all generators will deliver the same active and reactive power to the overall system. Modern power systems require modernization of all facets of power transmission. In smart grids, both current and new technology must be integrated in such a way that optimal performance is maintained.

Sensor networks must consider the physical structures, regulations, communication protocols, and data management. Centralized data independent of application has been proposed in order to eliminate data silos created by the lack of interaction between different sensor systems. In a centralized data structure, data sets are created dynamically. This shows overlapping data and underscores the interconnectivity of data across the grid. This need for a sensor network is critical given the proposed smart grid would have both distributed and centralized components,

“In this section, we re-structure the sensor/network/data collection head end/application stack by partitioning horizontally to group the sensors and communications

network into a single structure, and thereby separate the silos and decouple the applications from each other. This produces a *sensor network* for distribution grids that eliminates the need for exchange of sensor data among application systems and provides flexibility and scalability for both centralized and distributed systems. Multiple uses of field operational data are becoming increasingly necessary, and not just for AMI data as was depicted in Figure 3 above but for all kinds of grid and DER state data.” (Taft, pg. 4).

Advanced sensing and measurement have key goals for use in a smart grid. Sensor networks must be flexible, scalable, have communication structure, and a software platform that supports data flow. A sensor network which incorporates communication as a fundamental component makes interconnectivity and synchronization possible. Current sensors have multiple platforms in which data is aggregated. However, these platforms are not intertwined with one another. This creates lags in fault detection, fault recognition, and mitigation. Sensors capable of providing a continuous stream of data can be regulated with software data management. This provides continuous monitoring for the most vulnerable aspects of power grid infrastructure. For sensors without the capability of continuous streaming, communication protocols can collect sensor data in regular intervals much the way SCADA does. In this system existing SCADA and new software-based measurement techniques can be utilized on the same grid. Latency caused by data propagating between intermediate layers of software or transfer of data will be eliminated with a data centralization platform in which communication networks and sensors are operating together. [14]

Utilizing the best technology of the time power quality, sustainability, and reliability has been delivered to millions of people with the current power grid. This current power grid has been updated as new tools become available. The modern vision of a smart grid has many advantages. Customers will have the ability to actively participate in their power use. Smart monitors will give customers the ability to see their power use and peak time use. A smart grid will incorporate various types of electricity storage and generation. Independent power generation sources such as residential solar panel systems will have the ability to provide power to both the resident's home and the larger grid. A smart grid will have advanced features for greater power quality control. A smart grid will be able to respond quickly to changes in load and power delivery. This quality control will reduce current losses experienced by businesses and families that are dependent on sustained quality power. The current power grid loses power due to resistivity and reactance of transmission lines and electrical infrastructure. In the Department of Energy's vision of a smart grid, continuous monitoring will enable a self-healing grid [13]. A self-healing grid responds to faults and parameter changes instantly through continuous monitoring. This self-healing process is both preventative and reactive, "The self-healing grid will minimize disruption of service by employing modern technologies that can acquire data, execute decision-support algorithms, avert or limit interruptions, dynamically control the flow of power, and restore service quickly. Probabilistic risk assessments based on real-time measurements will identify the equipment, power plants, and lines most likely to fail." [10](Unknown, pg 7). Given the rising demands and complexities of a modern interconnected world, the smart grid has critical features and benefits for an increasing

population, more advanced network, dynamic energy needs, and environmental conservation efforts.

### Perovskite Optoelectronics

Perovskite crystals were first discovered in 1839 by Lev Von Perovski and Gustav Rose [15]. The crystal structure of perovskites is a face centered cubic lattice with a metallic element at its center. The corner Atoms are typically cations, while the face atoms of the cubic lattice are anions. Over the past decade, the optoelectronic properties of Perovskites in uses such as lasers and solar panels have been the subject of academic research. In this section we will deeply discuss the optical electrical properties of perovskites, the electrochemistry, perovskite solar cells, and fabrication techniques.

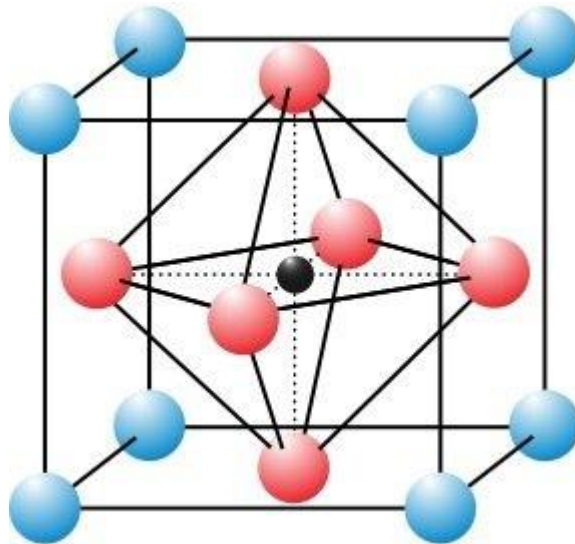


Figure 4: Perovskite crystal structure [15].

#### 1.2.5 Optical and Electrical Properties

Perovskites have garnered much attention from the scientific community for a decade. In this relatively short time, the power conversion efficiency of perovskite solar

cells has increased dramatically from 3.9% to 24.2% [16]. This trend can be seen in Figure 5.

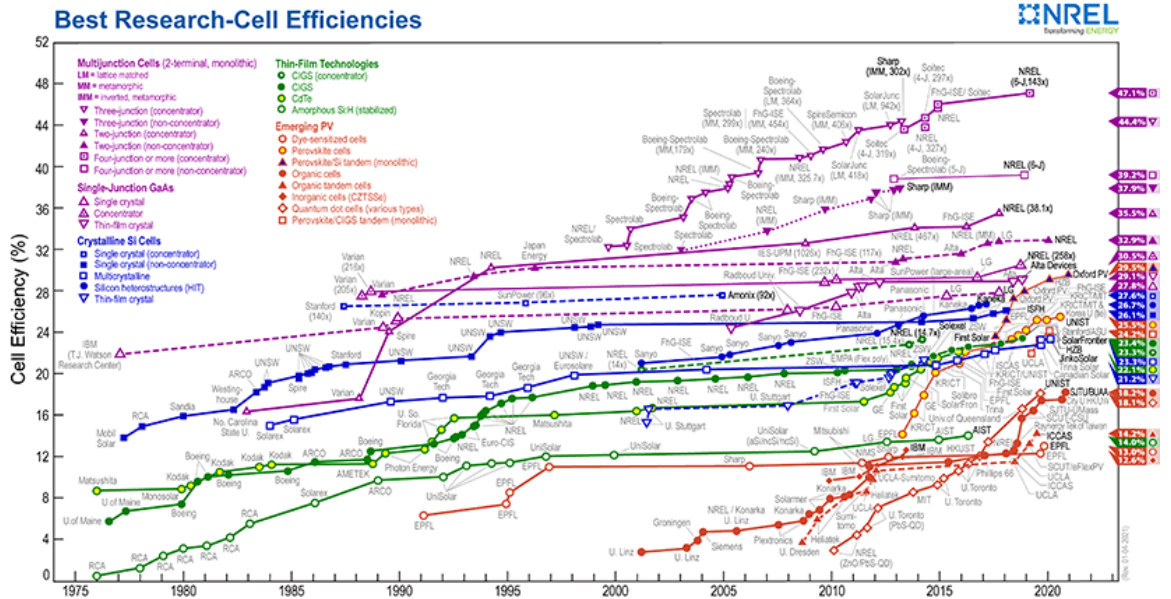


Figure 5: Power Conversion Efficiencies of various researched materials [16].

Perovskites have gained much attention for their high absorption rates across the visible spectrum, long charge diffusion lengths, and tunable bandgap. This high optical absorbance, which can be varied easily by tuning the bandgap, makes Perovskites an attractive material for solar panel applications [17]. Perovskites have attracted attention for their use in optoelectronics not only for their optical characteristics, but for their electrical characteristics. Perovskite crystals have been shown to have long carrier diffusion lengths. These characteristics of Perovskites attribute to their high power conversion efficiencies.

### 1.2.6 Electrochemistry

In this innovative research effort, numerous fields of science have crossed over to further third generation solar panels. Electrochemistry is the study of how chemical

processes cause electrons to move. In Perovskite Solar Cell (PSC) research electrochemistry is utilized to fabricate the precursor solution of perovskite (PSK) crystals. By varying the molarity of certain amounts of precursor chemicals, the electrical characteristics of the solar cell devices were modified. By utilizing a molar excess of lead iodine in a mixed cation Lead based Perovskite solar cell, higher open circuit voltage was achieved. This is because the excess lead iodine passivated the grain boundaries creating a conductive electrical channel in the Perovskite [18]. The use of inorganic salt additives in perovskite precursor solutions has shown to change the morphology of the crystal. This morphology has a tangible effect on the electrical characteristics of the crystal [19]. The relationship between the chemistry involved in Perovskite's fabrication and its characteristics is evident. Fabrication techniques such as spin coating have yielded an array of morphologies in subsequently an array of PCEs. For example, using the antisolvent method a perovskite precursor solution is spun coated onto a glass substrate. Then an antisolvent is deposited onto substrates to crystallize perovskite [20]. The research into the relationship between the chemical processes in the electrical processes of Perovskites is ongoing. Deeper insight into how the chemical reactions affect the quantum mechanical processes is required in order to gain a mastery over this technology.

### 1.2.7 Perovskite Solar Cells

The widespread use of solar energy has been abated due to certain challenges with silicon photovoltaic technology. Traditional silicon solar panels are more expensive than conventional fossil fuels. This is in part due to cost of materials required to fabricate and install these panels. With the effects of climate change creating a global crisis, alternative forms of energy are necessary. Perovskite solar cell technology has the potential to expedite

the widespread use of solar energy. Perovskite solar panels can be fabricated using relatively low cost materials reducing the overall cost to be comparable to conventional energy sources. Perovskite solar panels can also be fabricated using a number of processes. Using a solution deposition method, perovskites can be created using spin coating, slot die coating, roll to roll manufacturing, and spray coated easily [21]. This expands the range of substrates which can be used for solar panel fabrication. Solar panels fabricated on flexible substrates could be installed by rolling them onto a flat surface. This type of installation would further reduce the costs for transitioning to this alternative energy. The optoelectronic properties of perovskite crystals can be changed by varying the materials and amount of materials in the crystal. The band gap of perovskite crystal has been shown to vary with material selection [18]. This discovery shows the potential for creating silicon-perovskite tandem solar panels and multi layered perovskite solar panels with higher power conversion efficiencies. The increased use of SnO<sub>2</sub> as an electron transport layer has shown increases in power conversion efficiency. This is theorized to be due to the better energy level band alignment of perovskite crystals and Tin (IV) Oxide, deep conduction band, and high electron bulk mobility [22]. The hole transport material is organic layer doped with Lithium ions. In recent research efforts do use of a hole transport layer containing Spiro-OMeTAD has shown good thermal stability and increased power conversion efficiency. The metal electrode layer of n-i-p PSK device can be deposited via thermal evaporation. Thus far the results of this ongoing work have been promising.

Utilizing a mixed cation Perovskite, a power conversion efficiency of 17.01% was achieved. Perovskites which have used other techniques such as Lead excessing and mixed cations with the addition of inorganic salts have achieved PCEs >20% [18, 24]. The fill

factor increases as power conversion efficiency increases. It also maximizes the amount of energy delivered to the panel as opposed to being wasted via heat and reflection. Fill factor and power conversion efficiency typically increase in unison as the device is improved. This increase in power conversion efficiency not only is focused on the Perovskite layer, but on the other layers of the device. The effort to optimize the performance of PSC has many techniques and methodologies.

By enhancing the open circuit voltage and fill factor, the overall power conversion of the device becomes enhanced. In Chen's *Minimizing Voltage Losses in Perovskite Solar Cells*, many approaches are discussed. At the interfacial boundary of the perovskite and transport layers, energy band difference act as a source of voltage loss. Drastic differences in these energy bands further reduce the open circuit voltage by depleting the charge carriers at the interfaces [25]. A number of strategies to address this interfacial loss are being implemented. The use of different materials for the transport layers to reduce loss has shown promising results. Traditionally Titanium oxide nanoparticles have acted as an effective electron transport layer. However, the available energy levels of this material versus the energy levels of the perovskite crystal have a large disparity. Thus, it creates voltage loss in the device. Tin oxide nanoparticles have a better energy level band alignment with many perovskite crystals [22]. Tin oxide has also shown longevity in maintaining the power conversion efficiency after one thousand hours of operation. This can be seen in the data of Figure 6.



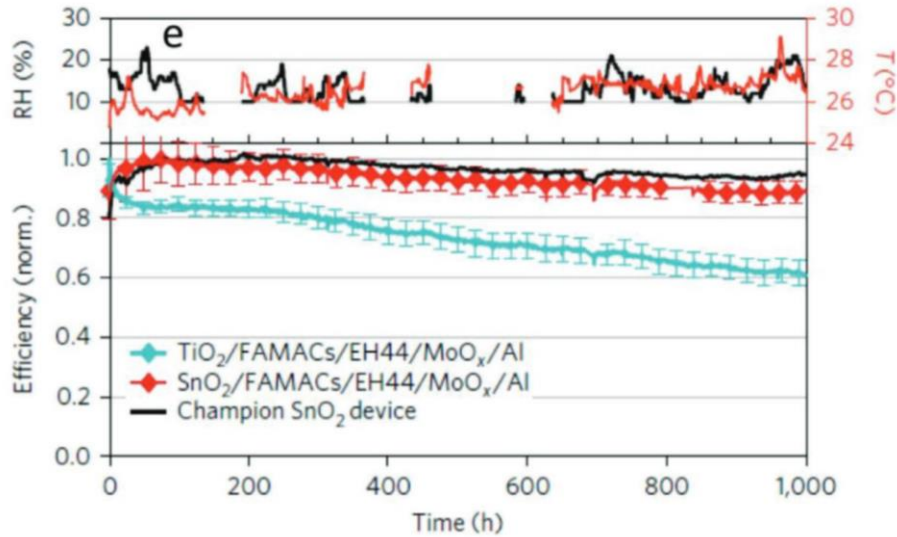


Figure 6 1: The power conversion efficiency of solar cells with titanium oxide and tin oxide over one thousand hours [22].

Tin oxide was shown to have superior stability under UV light than Titanium oxide. This causes better preservation of the original the original power conversion. Tin oxide as an ETL, has reduced the hysteresis between the forward and reverse scans of the device.

The morphology of the cell plays a large role in the operating parameters of the device. The morphology of the cell not only determines physical qualities such as stability and degradation time, but it also impacts the electrical behavior of the device. Perovskites typically are tolerant to defects in the device such as cracks, pinhole defects, and scratches. These defects however act as recombination sites. The majority of nonradiative recombination occurs in trap assisted states at defects in the perovskite [25]. This recombination in the defects' attributes to the majority of voltage loss in the perovskite. Perovskites which have a high degree of defects typically have low open circuit voltage. These defects can happen in the fabrication stage of the perovskite. The perovskite is sensitive to environmental conditions such as humidity, temperature, oxygen content, and

fabrication factors such as drop time of antisolvent [18]. Minimization of defects is critical to the minimization of non-radiative recombination. Other types of defects such as pinholes have been shown to affect the quality of perovskite solar cell operation as well. Along with incomplete surface coverage of perovskite that pinholes produce, pinholes in the perovskite have an adverse effect on the short circuit current of the device [26]. Pinholes act as conduits between layers of the device which are supposed to be separate. For example, Holes in the HTL and electrons from the ETL can recombine prematurely in the device. This reduction in electrical work is highly undesirable. Pinholes also reduce the absorption of light by the perovskite. The holes act as centers for reflection and diffraction. This parasitic reflection if not considered, skewed analysis of the behavior of the device creates imprecise conclusions for some perovskites and on this innovative technology as a whole.

Recombination in the perovskite has many sites within the bulk of the crystal. Grain boundaries act as a source of recombination in the device as electron-hole pairs are photogenerated. The grain boundaries vary with the grain size itself. Perovskites with smaller grains have far more grain boundaries than perovskites with larger grain sizes. Passivation of defects and recombination sites at these boundaries is a major area of perovskite solar cell research. By using excess amounts of ions, grain boundaries become electrically conductive. Therefore, grain boundaries no longer act as a site of undesirable recombination. The excess ions gather between perovskite grains and transport charges from the bulk crystal to the transport layers. By passivating these defects both at the grain boundaries and in the bulk of the crystal with excess ions, a high photoluminescence quantum yield. More of the optical energy is converted into electrical energy. Cations such as potassium and halides at grain boundaries and surfaces lowers the non-radiative

recombination in perovskites [22]. This yield provides the most area of growth via research and development. This excessing of ions increases the density of grain boundaries and increases the photogenerated carrier lifetime [27]. Ions with smaller ionic radii typically coalesce at the grain boundaries [22]. This passivation has been shown to increase open circuit voltage.

### Simulation and Modeling

Perovskite solar cell technology has the potential to expedite the widespread use of solar energy. Perovskite solar panels can be fabricated using relatively low cost materials reducing the overall cost to be comparable to conventional energy sources. Perovskite solar panels can also be fabricated using a number of processes. The main factor in perovskite solar cells which make them a viable candidate for energy production is the ease with which the optical properties can be changed. Properties such as band gap, lattice constant, morphology, charge carrier lengths, power conversion efficiency, fill factor, open circuit voltage, and short circuit current can be adjusted by varying the precursor chemistry for the crystal. While varying the chemical composition of known perovskites has shown positive developments, there are thousands of perovskites with various opto-electronic properties. Fabricating and testing every combination of perovskites is infeasible and highly expensive. The use of simulation and modeling tools to develop perovskites has proven to be highly effective and powerful. Simulation techniques such as software development, block diagram modeling, and machine learning (ML) have given researchers the tools to develop props guys with speed and accuracy previously unavailable.

### 1.2.8 Machine Learning

ML applies the concepts of Artificial Intelligence (AI) to data processing. ML is an algorithm or set of algorithms that allows the computer to automatically learn and improve calculations. This self-improving structure does not require tedious reprogramming in order to become more accurate and precise. A machine learns by observing data and ascertaining patterns in the data set. With these patterns and trends, new information can be analyzed far more efficiently. There are many methods of machine learning such as Support Vector Regression, Artificial Neural Networks, and Random Forest. These mechanisms of machine learning are currently being used in the development of perovskite solar cells for higher efficiency, material science analysis, and modeling of the quantum mechanics in the perovskite crystals. ML in perovskite solar cell research has many useful applications. ML currently is being used to predict the electrical and optical properties of metal halide perovskite which have not yet been directly experimented with in a lab.[3] By using this technique of discovering and narrowing down the range of possible perovskites for solar panel application, a more focused effort testing a range promising materials will expedite the development of this technology.

Neural networks are a powerful tool in ML. By using a set of variables and constraints, a machine can process trends, describe behavior, and predict properties based on the network's output on inputted data. ML structural and electronic properties of metal halide perovskites using a hierarchical convolutional neural network were studied in [28]. They use a neural network which predicts the electrical properties of perovskites based on preset parameters categorized into different groups. The descriptor groups elemental,

precursor based, and  $ABX_3$  based coalesce the important factors in the quality of perovskite solar cells. With these descriptor groups as inputs into the neural network, the researchers were able to great accurate results. The work associates the chemical and physical properties of the cells with the electrical and optical properties in order to cite patterns. The focus of the paper is to vary the organic component of the perovskites. Organic electronics are of particular interest because of their good thermal stability, humidity tolerance, and in some devices complex impedance surface [29]. By varying the organic element of the perovskite, materials with these properties which have not been tested yet could be predicted. Thereby focusing the research efforts to be scientifically and cost effective.

In this approach, certain presumptions of perovskites were kept constant in order to keep the fundamental properties of the crystal. The lattice, inorganic structure of the perovskite, and odd number of electrons per unit cell kept the nonmetallic properties of the crystal and enabled the predictions to be accurate. The network was able to correctly calculate the bandgap of the perovskites of various organic and inorganic combinations. The elemental group of constraints in the network factored the first and second ionization energies and electron affinities. These factors are highly influential in the crystal's bandgap. The precursor based group considered the chemicals required to fabricate the solution. For example,  $MAPbI_3$  can be fabricated using precursor solutions MAI and  $PbI_2$  dissolved in a medium. The precursor based group is important to capture the chemistry of the perovskite and were deemed important by the research team. The configuration of these elements in the perovskite such as the lattice constant and metal-halide-metal octahedral tilt angle have a profound effect on the optical and chemical properties of the crystal.

The scheme of the Convolutional Neural Network (CNN) employs a 1 x N input vector containing the number of features of the perovskite. This vector first passes through a 1D convolutional layer containing 64 filters. The data is filtered by processing it with the kernels of each 1D filter. The output is then filtered into a 2D containing 128 filters with a 2D kernel. Each 2D filter is comprised of five rows and columns matching the number of input features. The processing of both of these layers yields the same size vector as the input. The neuron layer has 100 hidden neurons performing elementwise rectified linear activation. The output of the neurons is a calculation of the bandgap for that material. To mitigate possible human error and bias, 80% of the data is selected randomly as input.

The inner device physics of perovskites has a profound impact on the power conversion of the cell as a whole. Predictions and strategies learned from ML to develop high-performance perovskite solar cells are investigated in [30]. The factors of power conversion efficiency are analyzed from a device level perspective. The differential between the perovskite and the hole transport and electron transport layer are critical for the device's power conversion efficiency.

This work attempts to use various ML techniques to correlate the properties of the layers of a solar cell device, the properties of the crystal, and the power conversion efficiency. The researchers used different types of machine learning and analyzed the root mean square error to ascertain which one was most accurate. The error is calculated using equation 4.

$$\sqrt{\frac{\sum_{i=1}^N (x - \dot{x})^2}{N}} \dots\dots\dots(4)$$

Their results showed the artificial neural network to have the least root mean square error in its predictions of Power Conversion Efficiency (PCE). The correlation factor can be calculated using equation 5.

$$\frac{\sum_{i=1}^N (x-\bar{x})(y-\bar{y})}{\sqrt{\sum_{i=1}^N (x-\bar{x}) \sum_{i=1}^N (y-\bar{y})}} \dots\dots\dots(5)$$

The artificial neural network showed a high correlation factor. However, the ANN did not have the highest correlation. The K Nearest Neighbors (KNN) and Random Forest (RF) algorithms had the highest correlation between data and predictions. This indicates that different techniques have different strengths and weaknesses. The researchers omitted duplicate data in order to avoid non-uniform distribution. This device oriented analysis examines the complex physics of a perovskite solar cell device. These results can be used to direct further investigation into materials with better energy alignment with the perovskite crystal. Large differences in energy bands act as a source of energy loss in the device. This ultimately diminishes the overall PCE of the device irrespective of the quality of the perovskite crystal. This approach was able to accurately learn the properties of the crystal and device such that new materials were predicted.

The built model was tested by designing new set of perovskite materials with predicted bandgaps. The bandgaps were predicted utilizing their chemical properties and composition. This predicted crystal behavior was tested by synthesizing the perovskites and comparing the results. The perovskites tested were  $Cs_xMA_{1-x}PbI_3$ ,  $CsPb(I_xBr_{1-x})_3$  ,

MAPb<sub>1-x</sub>Sn<sub>x</sub>I<sub>3</sub> with different ratio values of x predicted from the machine learning algorithm. The results of the bandgaps ranged from 1.3-2.3 eV. The experimental results of the crystals were 1.4 eV (MAPb<sub>1-x</sub>Sn<sub>x</sub>I<sub>3</sub>), ~1.8 eV (CsPb(I<sub>x</sub>Br<sub>1-x</sub>)<sub>3</sub>), and 1.4 – 1.8 eV (Cs<sub>x</sub>MA<sub>1-x</sub>PbI<sub>3</sub>). Other ternary perovskites such as MASnI<sub>3</sub>, FASnI<sub>3</sub>, and CsSnI<sub>3</sub> were tested for accuracy of non-mixed metal and non-mixed halide perovskites. The predicted bandgaps for MASnI<sub>3</sub> and FASnI<sub>3</sub>, which were in the dataset, were 1.36 eV and 1.38 eV respectively. The fabricated samples showed band gaps of 1.37 eV (MASnI<sub>3</sub>) and 1.4 eV (FASnI<sub>3</sub>). The fabricated CsSnI<sub>3</sub> was predicted to have a bandgap of 1.15 eV. The fabricated sample had a bandgap of 1.25 eV. This result is especially significant because this perovskite was not in the dataset. This demonstrates the ANN not only can accurately tell the bandgap of known materials, but also unknown materials which have not been feed into the system. The random forest algorithm also was able to predict bandgaps of different materials with accuracy.

In Li's work, random forest machine learning was also implemented to test the algorithm's accuracy in learning and predicting bandgaps of perovskites. Random forest learns data patterns by interconnecting data in growing hierarchal trees. These trees are built from the outermost branches to the innermost branches. This tree is then verified from the bottom up for accuracy [31]. This method of spatial clustering can also predict new materials not a part of the dataset. However, because of the limitations of the random forest algorithm, the artificial neural network worked the best for this application.

The algorithms attempted to predict other important factors about the solar cell such as short circuit current, open circuit voltage, maximum power point, and fill factor. The results of both the ANN and Random Forest algorithm had a correlation factor less than



0.5. This means the predicted results were not accurate and showed a relatively large divergence from measured results. Neither model factored in metal electrode contacts and conductive back contacts. These factors were not incorporated into the model's input parameters. These results also yielded a large root mean square error for the results. While this model can't accurately predict these values, it further demonstrates that these parameters of the device are critical for optimizing the performance of the solar cell device.

This innovative research has many potential benefits. ML for perovskite solar cells has many applications for researchers to explore. The critical aspects of solar cells such as fill factor, power conversion efficiency, open circuit voltage, short circuit voltage, and maximum power point can be accurately predicted and analyzed to simulate perovskite without necessitating expensive laboratory equipment and intricate fabrication processes.

#### 1.2.9 Data Analytics

The inner mechanisms of this Perovskite optoelectronics remain the topic of research. The ideality factor of these devices gives insight to the possible recombination mechanisms within the device. The ideality factor gives indications of loss due to recombination and charge carrier diffusion lengths [32]. Minimizing losses from recombination will increase both open circuit voltage and power conversion efficiency. Optimizing these factors are key to making this third-generation solar cell technology sustainable for public consumption. By observing the resulting ideality factors of fabricated perovskites, trends in the electrochemistry and recombination can be ascertained. These trends establish a relationship between the perovskite crystal's chemical composition and optoelectronic properties, interfacial recombination mechanisms, and sources of non-radiative loss. Because there are thousands of different types of perovskite and numerous

compositions for hole and electron transport layers, it would be infeasible to fabricate and test every combination of perovskite and transport layer pairings. Analyzing these solar cells with respect to their ideality factor would expedite optimal combinations and shed light on how these layers are interacting with each other.

Fabricating perovskite crystals is a multistep process which requires various low-cost materials. The morphology and composition of the perovskite are controlled utilizing both chemical and mechanical processes. Using a mixed halide perovskite, the optical band gap is controlled for optimal performance. This level of control from the fabrication process gives the designer the ability to modify device behavior [29]. The perovskite crystal is fabricated using the one-step solution method. A precursor solution containing  $\text{PbI}_2$ ,  $\text{PbBr}_2$ , Sigma Aldrich Dimethyl Sulfoxide anhydrous  $\geq 99.9\%$  (DMSO), and Sigma Aldrich Dimethyl Sulfoxide anhydrous  $\geq 99.8\%$  Dimethyl Formamide (DMF), Sigma Aldrich Methylammonium Iodine (MAI), and Sigma Aldrich Cesium Iodine additive. The electron transport layer is formed by spin coating an aqueous solution of Tin (IV) oxide nanoparticles on to a glass substrate containing Fluorinated Tin Oxide (FTO) and annealing at 100 C. This stoichiometric mixture has a molar excess of Iodine mixing  $\text{PbI}_3$ ,  $\text{PbBr}_3$ , and MAI in a solvent of DMF and DMSO. CsI is then added to control morphological characteristics and electronic properties. The morphology of the perovskite crystal containing inorganic salts such as cesium had a different crystal lattice than perovskite without any added salts [8]. A Sigma Aldrich Chlorobenzene (CBZ) antisolvent is dropped on to a spinning sample to remove the DMSO and DMF leaving only the perovskite compounds necessary. Annealing is done in the inert environment devoid of humidity. The annealing crystallization process leaves  $\text{Cs}_{0.05}(\text{MA}_{0.17}\text{FA}_{0.83})_{0.95}\text{Pb}(\text{I}_{0.83}\text{Br}_{0.17})_3$  perovskite

nanocrystals. The average grain size of the nanocrystals is controlled predominately by the antisolvent deposition process. By testing the fabricated samples utilizing a solar simulator, the resulting current voltage relationship can be seen of lab made perovskite solar cells. Using a custom program, the ideality factor of these lab made samples can be ascertained. this will lead to a better understanding of the inner quantum mechanics of perovskite solar cells.

The ideal diode is a perfect semiconductor device whose properties allow current above a desired voltage. This behavior acts as a switch in a circuit allowing current flow in one direction. In the reverse bias direction, the diode does not allow current to flow. Such a device is theoretically impossible due to the quantum mechanics of the PN junction. The PN junction is the boundary between positively doped and negatively doped semiconductor material. In an ideal PN junction, the only mechanism of recombination is direct electron hole recombination. In an actual diode, recombination occurs due to drift of hole and electrons and other higher order recombination mechanisms causing a leakage current. Typically, bimolecular recombination gives a unit ideality factor and are radiative. In contrast, trap assisted recombination is typically non-radiative and has an impact on ideality factor and device performance [33]. These second and third order recombination mechanisms yield an ideality factor greater than one thereby deviating from the theoretical ideal model.

Using the ideality factor to analyze the inner recombination mechanisms of fabricated perovskite solar cells, the quantum mechanics in the cell can be accurately assessed. By accurately attaining the ideality factor using data analytics, the statistical analysis of this new technology can direct the fabrication process. Statistical analysis can

identify possible errors in the experimentation, optimal points for concentration of materials, and the best fabrication method to utilize. Utilizing data analytics, the quantum mechanics of perovskites can be mastered. With this mastery the proliferation of Perovskite solar panels and subsequently sustainable solar energy can direct global power infrastructure to a more environmentally conscious future.

## CHAPTER 2. BACKGROUND OF PEROVSKITE RESEARCH

Perovskite research has yielded very promising results. The rapid improvement in power conversion efficiencies of perovskites has increased in a relatively short time unlike many other projects. In this section the overall status of perovskites solar cell research will be discussed. Because this emerging technology is so new, new materials for electron transport layers have to be considered in order to optimize device performance. There are thousands of different types of Perovskites. While it is infeasible to test and experiment with every possible combination of prospect crystal there have been certain candidates which have shown more development than others. The progress of perovskite crystal growth, improving morphology, and the inclusion of additives to enhance the quality of this crystal are currently the subject of many laboratories research. The use of different materials in the hole transport layer is currently the subject of research as well. Research based on the interfacial boundary between perovskites and transport layers is based on the issue of energy level band alignments. Efforts to improve energy level band alignments between perovskites in subsequent layers is the focus of research in order to increase power conversion efficiency.

### Electron Transport Layer

The electron transport layer of a solar cell is the layer which extracts the electrons from the intrinsic semiconductor. This layer must actively reject holes produced by the semiconductor optical absorber, and effectively conduct electrons away from the intrinsic layer. For n-i-p solar cells this layer is deposited on top of these substrates. For an inverted

p-i-n solar cell, this layer is deposited atop of the optical absorber. In a p-i-n architecture, the electron transport layer also serves as a moisture barrier to prevent outside water from penetrating the device. For perovskite solar cells, even for solar cells utilizing the same type of crystal depending on the architecture the composition of this electron transport layer can be dramatically different. This is due to the electron transport layer's ability to withstand higher temperatures than the crystal. The type of deposition method for the electron transport layer also has an effect on the choice of materials to use in fabrication. Deposition methods such as spin coating, blade coating, printing, and slot die coating have unique pros and cons which affect the performance of the device. Typically, the electron transport layer of perovskite devices are inorganic metal oxides. The most popular metal oxides are  $\text{TiO}_2$ ,  $\text{SnO}_2$ , and  $\text{ZnO}$  [22]. Titanium oxide has a longstanding reputation of being an effective electron transport layer. However, issues such as degradation would expose the UV light has pushed the need for the exploration of new materials. Titanium oxide also has many oxygen-produced vacancies causing poor contact at the interfacial barrier. These defects at the interfacial boundary cause premature recombination of electrons [34]. Tin oxide has better energy level band alignment with mixed cation perovskites. With better energy level band alignment, quasi fermi level splitting is less dramatic. This causes photogenerated electrons to not prematurely recombine at this interfacial surface of the electron transport layer and the perovskite. These metal oxides have a wide bandgap energy making them transparent to visible light. In [34] it was found that the solvents in which the  $\text{SnO}_2$  particles were dissolved in had an impact on the formation of the electron transport layer. This subsequently impacted the performance of the overall device. This works succinctly illustrates how critical this layer is to the overall

power conversion efficiency of perovskite solar cells. Do use of additives in tin oxide electron transport layers is being explored as a possible option to increased power conversion efficiency. By contrasting two solar cells, one with a tin oxide layer verses a tin oxide layer fabricated with phosphoric acid, the differences in performance can be seen. The solar cells with a phosphate tin oxide ETL showed higher power conversion efficiency then the electron transport layer made of tin oxide. While turn oxide nanoparticles are commercially available, some research Utilizing fabricated tin oxide nanoparticles is ongoing [35]. The preparation of tin oxide unit particles utilizing tin chloride nanoparticles exposed to UV radiation has yielded very interesting results. The research team found an optimal point of 60 minutes of UV light exposure. This implicates a positive role that chlorine ions could play in a tin oxide nanoparticle electron transport layer. Given the vast amounts in wide scope of research in effective electron transport layers for perovskite solar cells, the critical role this layer please in the overall function of the device cannot be underestimated.

#### Perovskite Optical Absorption Layer

Perovskites have made tremendous progress over the past decade. Since 2009 the power conversion efficiency of perovskite solar cells has jumped from 3.9% to 24.2% in the span of a decade [36]. This much improvement in such a short time frame has garnered perovskite solar cells much attention from the scientific community. While this innovative technology has shown much promise, there are still short comings which make it unsuitable for commercial use. This is the basis of research in power conversion optimization research.

Within the perovskite crystal, numerous different types of recombination occur. Bimolecular recombination, non-radiative trap assisted recombination, and Auger recombination are some of the predominate types of recombination to occur in these crystals. In an ideal case, only radiative recombination would occur and contribute to the overall desirable properties of perovskite. However non-radiative recombination diminishes the power conversion efficiency of the crystal. Mid gap traps in the energy band of the perovskite act as recombination sites. Physical properties of the crystal have an affect on the electrical properties. The morphology, crystallinity, and defect in the physical structure of the perovskite can hinder or enhance electrical properties such as open circuit voltage, short circuit current, and ideality factor. There are currently a number of approaches to improving the electrical properties of the perovskite by chemical and mechanical means. Maximization of open circuit voltage is a popular approach to optimization of perovskite devices [37]. In this approach sources of voltage loss from physical, chemical, and quantum mechanical means are explored. The use of chemical additives to improve the quality of the perovskite crystal have shown promising results [25]. Grain boundaries have been shown to act as sites for recombination. Passivation of these sites to optimize radiative recombination the precursor solution is manipulated in have a stoichiometric surplus of a particular anion or cation [27]. Another electrochemical approach to improving the electrical properties of perovskite is addition of inorganic salts to change the morphology [38].

The physical characteristics and electrical characteristics of the crystal have been proven to be connected. A particular equation explaining the exact relationship between grain size, defect concentration, and other physical properties and the electrical



characteristics has yet to be derived. For instance, how the voltage reduces with the concentration and length of micro cracks is not known. Pin hole defects which reduce the short circuit current can be interpolated with further research on how they are formed, and depth must be investigated. The physical parameters of these defects have as much of an impact on device performance as the physical parameters of the crystal. The spin coating method has produced low defect perovskites. This method is not suitable for manufacturing and production. Other manufacturing methods such as slot die coating, printing, dip coating, and chemical vapor deposition have created other issues in the quality of the perovskite. Why this is and the concentration of defects must be investigated in order to find the best method of fabrication which is scalable. Once said techniques are found, it must then be optimized in order for reliability and maintainability of high-quality perovskite solar cells.

The use of additives in fabricating perovskite solar cells has shown much promise. In fabricating Formamidium based perovskite solar cells, additives such as methylammonium Chloride (MACl) and methylammonium Bromine (MABr) improve the crystallinity, morphology, and overall device performance [39]. Inorganic salts such as cesium can be used to create a triple cation site in order to enhance morphology and performance [38]. Inorganic salts such as Cesium and Rubidium have changed morphology of perovskite crystals. Results indicate this is because of the smaller atomic radii size. This is a novel approach to morphological control of perovskite solar cells because of the ease with which optimal points can be identified. Research labs can simply vary the concentration of inorganic salt additives in order to see how these salts affect nanostructure. Imaging techniques such as X Ray diffraction and scanning electron

microscope can get insights into how these salts affect the grain size in grain boundaries within the perovskite crystal. That has been shown that these boundaries in this grain size play a critical role in the overall optoelectronic properties of the perovskite. Therefore some research labs have made this the focus of their efforts to improve perovskite's optoelectronic performance.

The stoichiometric precursor solution involved in fabricating perovskites is complex and very sensitive to environmental conditions. The chemical compounds involved and solvents in which they are dissolved play a critical role in the end results of the device. The molarity of the material in the precursor solution has to match similarity of the end formula of the perovskites. However, some results have shown that accessing certain precursor solutions can have positive effects on device performance. For instance, utilizing the excess of lead iodide in a MAI perovskite, has shown to passivate grain boundaries which acts as a site of nonradiative recombination. While progress has been made there are still issues to address before commercially available perovskite solar panels can be a reality.

#### Hole Transport Layer

The hole transport layer extracts holes from the perovskite to act as charge carriers. This layer must be tolerant to humidity and atmosphere conditions for a n-i-p structure. For a p-i-n structure, the composition of this layer may be totally different. This layer, and the interfacial boundary it creates with the perovskite, is critical to the functioning of the device. There's ongoing research into the use of organic materials to fabricate this layer of the device. Organic electronics have drawn much attention because of their high thermal stability. This layer acts as the intermediary between the perovskite layer and the metal

electrode. Much like the electron transport layer, considerations of the energy bands alignment with the perovskite's energy bands must be taken into consideration.

In [40] research studies, the hole transport material is organic layer doped with Lithium ions. The organic layer containing Spiro-OMeTAD has been shown to have good thermal stability and increases power conversion efficiency. This layer is spin coated on top of the perovskite crystal and left for twenty four hours to allow Li doping in a dark and inert environment. This step is critical as this layer is also sensitive to environmental conditions such as humidity and light. This work has intellectual merits and is likely to produce viable results. Utilizing material proven to increase power conversion efficiency, this work is likely to yield promising results.

The energy level bands represents the difference in the highest occupied molecular orbital (HOMO) and lowest unoccupied molecular orbital (LUMO). Between these two levels excitation is most likely to occur. Therefore, when energy bands are most aligned the coinciding region in which excitations can occur is maximized. In the converse, when energy level bands are poorly aligned this minimizes the region in which excitation can occur between energy level bands. These energy level bands can be ascertained quickly and easily via the chemical composition of the fabricated layer and computational analysis tools [41]. This computational study is valuable because ascertaining energy bands before fabrication can better illuminate compatible pairs between HTM and perovskite crystals. Having a large degree of energy level band overlap is critical to the power conversion efficiency of the device. Misaligned energy level bands allow charges to build at the interfacial boundary. This charge buildup is the primary cause of premature recombination. Devices with low power conversion efficiencies have a high degree of these parasitic

recombinations. Given the fact this study analyzed the energy band diagrams of many small molecule HTL materials commonly used in solar cell fabrication, this is a valuable contribution to the research of perovskite solar cells. This study can expedite the research into high efficiency perovskite solar cells. With materials of similar energy level bands paired, PCE is sure to increase easily.

The use of additives in electrochemistry to modify behavior has been shown to be effective. much like in the prostate layer the use of additives in enhanced conductivity or modified bandgap. In there the use of doped layers has been shown to have positive effects on power efficiency. Used in a p-i-n structure, a nickel oxide composite hole transport layer doped with copper has shown to enhance charge transport [42]. The composite HTL utilized a doped layer of nickel oxide and poly(3,4-ethylenedioxythiophene) polystyrene sulfonate (PEDOT:PSS) showed better energy level band alignment. With better alignment hole collection and transport efficiency are increased. The chemical structure of the materials used in the HTL determine the energy level band, charge mobility, and the stability of the layer. These chemical factors determine which type of material would be best for which architecture. By analyzing the chemical structure of hole transport materials such as Spiro-OMeTAD and its derivatives additives and better compounds for this layer can be discovered. The charge transports of these particular molecules have a profound impact on the current produced by the device [43]. These devices also showed greater stability over operation time. This feature is critical for the commercial use of perovskites as degradation has been an issue. This work has yielded novel results which have positive implications for the use of additives to control optical and electrical characteristics. The

use of a copper doped nickel oxide composite HTL is good for the performance of the device and commercially viable.

## CHAPTER 3. METHODOLOGY

### Semiconductor Fabrication

Semiconductor fabrication is a complex multistep process. Any error at any step of this process can cause dramatic effects on the end result. This fabrication process involves both chemical and mechanical processes. Typically, PSCs are fabricated using the solution based method. This method involves creating a precursor solution from which the perovskite crystallizes. Current research is looking into variations in the mechanical fabrication process in order to make PSCs manufacturable. Production techniques such as slot die coating and printing can meet commercial demands. In this section the methodology of fabrication is outlined. This section is organized by substrate cleaning, tin oxide nanoparticle deposition, perovskite fabrication, hole transport layer, and metal electrode deposition. The resulting PSCs have the structure of figure 7.



Figure 7: The layers of the fabricated device. The bottom layer, deposited first, is the electron transport layer comprised of Tin (IV) Oxide nanoparticles, Perovskite crystal of  $\text{Cs}_{0.05}(\text{MA}_{0.17}\text{FA}_{0.83})_{0.95}\text{Pb}(\text{I}_{0.83}\text{Br}_{0.17})_3$ , Organic Hole transport layer, top electrode of gold.

Figure 7 1: The layers of the fabricated device. The bottom layer, deposited first, is the electron transport layer comprised of Tin (IV) Oxide nanoparticles, Perovskite crystal of  $\text{Cs}_{0.05}(\text{MA}_{0.17}\text{FA}_{0.83})_{0.95}\text{Pb}(\text{I}_{0.83}\text{Br}_{0.17})_3$ , Organic Hole transport layer, top electrode of gold.

### Substrate Cleaning

The substrate cleaning, though it may seem trivial, is vital to the proper fabrication of the PSC. The substrate must be clean to prevent any extraneous chemical reactions or physical defects caused by debris. These samples are also marked for data tracking purposes. The following experimental procedure must be followed precisely.

From the square of 3 x 3 FTO (ITO) substrates, break off a square along the etched lines. With the multimeter test resistance of the substrate. A nonconductive surface of 0.L will display as seen in Figure 8. There is no specified value of resistance for the FTO (ITO), any sign of any connectivity indicates the correct side. Take note, the two rectangular

sections on the substrate should not be conductive on the FTO (ITO) side. On the nonconducting side, an identifying number or letter in the bottom left corner is etched using a glass scratcher. This identifying mark should not be large as it will interfere with optical absorption. Once FTO (ITO) side has been identified and glass has been marked, place sample in petri dish FTO (ITO) side up. It is critical that the FTO (ITO) side not be placed face down at any point in the cleaning process. Using a mixture of tap water and Valconox Liquinox cleaning detergent in one beaker, deionized (DI) water and Valconox Liquinox cleaning detergent in another beaker, and Texwipe chemical wipes clean samples first using tap water soap mixture then DI water soap mixture. Once samples are cleaned with the DI water soap mixture, they should be rinsed thoroughly with DI water. Clean samples should be placed in a fresh Petri dish filled with DI water. The cleaning station should be set up as seen in Figure 9.

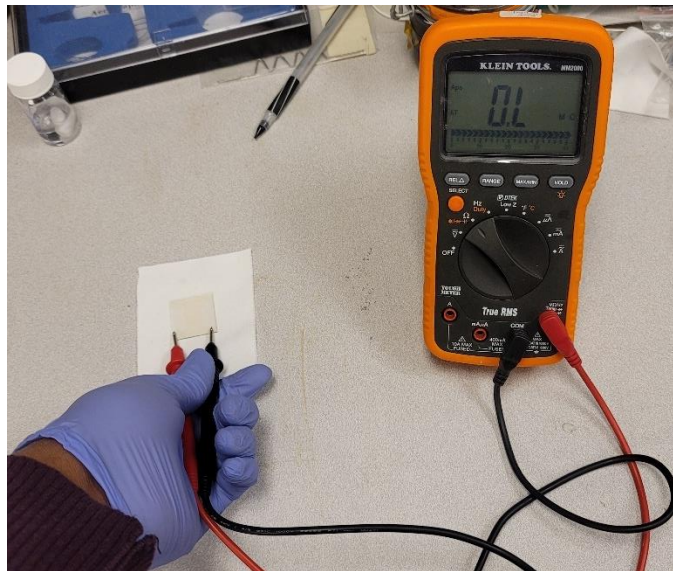


Figure 8: Multimeter reading of glass surface.



Figure 9 1: Water cleaning station.

Fill a glass cell holder with acetone. Using a chemical wipe, clean the substrates with acetone over a waste beaker. Thoroughly clean substrates with acetone and wipe and place the samples in the holding container filled with acetone with the FTO (ITO) side facing one direction. Please sample holder in beaker. Add water to be beaker such that the sample holder is slightly floating. In the digital pro digital ultrasonic cleaner, add water until beaker containing be sample holder is slightly floating. Set temperature to 50 degrees Celsius and set timer to 15 minutes. When the water reaches a temperature of 50 degrees and the acetone cleaning is complete, place beaker in water for ultrasonic cleaning. Repeat cleaning process for isopropanol alcohol. If substrate holder is not closed such that only the holder can be filled with alcohol, fill holder and beaker until samples are completely covered with alcohol. After alcohol ultrasonic cleaning, blow samples immediately with nitrogen gas to remove all traces of alcohol. This must be done to prevent with residual film from forming on to samples. Place clean samples FTO (ITO) side up into freshly opened clean petri dishes.



## Tin (IV) Oxide Deposition

The Tin (IV) Oxide nanoparticle electron transport layer is deposited by spin coating and annealing. This electron transport layer is critical to the device performance and can be quality tested to ensure proper fabrication. This fabrication process involves an aqueous solution of tin oxide nanoparticles, a spin coater, and a hot plate. The quality testing of this layer involves an electrical multi meter to test resistance.

Using equation 11, the amounts of Alfa Aesar Tin Oxide solution is given for 2.67% by weight (SnO<sub>2</sub>wt) of tin oxide in DI water given the concentration of the stock (C<sub>STOCK</sub>) is labeled on the bottle. The concentration of the Alfa Aesar solution is 20% tin oxide suspended in water.

$$\text{SnO}_2\text{wt} = 2.67\% * 2\text{mL} \dots\dots\dots(10)$$

$$\text{Solution Amount} = \frac{\text{SnO}_2\text{wt}}{C_{\text{STOCK}}} \dots\dots\dots(11)$$

$$\text{DI Water amount} = 2 \text{ mL} - \text{solution amount} \dots\dots\dots(12)$$

First, using the UV ozone cleaner pictured in figure 10, clean substrates for 15 minutes. Within 15 minutes of UV ozone cleaning, place samples on Chemat Technology KW-4A spin coater. Using 1000 microliter (uL) pipettes administer 110 uL of tin oxide solution on top of substrate. Set the spin coater to 3000 RPM. Press control, then vacuum, and then start to begin spin coating. Spin samples for 30 seconds. Place samples with spun coated nanoparticles on plate beside spin coder until all samples are done. Once all samples have SnO<sub>2</sub> on then, place on hot plate preheated it to 100° Celsius. Cover samples with glass cover slightly ajar. Leave samples to anneal for 30 minutes in outside air. Once annealing

is finished, quality check samples using multi meter. The multimeter should register ~20 ohms as seen in figure 11.



Figure 10: UV Ozone cleaner required.



Figure 11 1: Resistance of quality electron transport layer of Tin (IV) Oxide nanoparticles on FTO.

### Perovskite Crystal Fabrication

The precursor solution for the perovskite is made with a stoichiometric chemical process. Using the quantities listed in table 1.1, weigh in a 2 mL (at minimum) vial lead iodine ( $\text{PbI}_2$ ) and lead bromine ( $\text{PbBr}_2$ ). After weighing, add dimethyl sulfoxide (DMSO) and N,N-Dimethylformamide (DMF) in a 1:5 ratio respectively. If not already created, fabricate a stock solution of Cesium Iodine (CsI) dissolved in DMSO. The correct ratio of CsI and DMSO is 1 gram (g) to 2.566 mL of DMSO. Add 5% by volume CsI in DMSO. The  $\text{PbI}_2/\text{PbBr}_2$  mixture is placed on a hot plate stirrer at  $150^\circ\text{C}$  for 15 minutes. In this vial, weigh methylammonium bromine (MABr) and formamidium iodine (FAI). Place on hot plate stirrer at  $65\text{C}$  for two to three hours. This precursor solution must be made in a nitrogen filled glove box. The water contents inside the box must not exceed 5 PPM. the oxygen contents of the box must not exceed 10 PPM.

Table 1.1 Perovskite precursor solution materials and weights

Material	Amount
$\text{PbI}_2$	676.4 mg
$\text{PbBr}_2$	110.4 mg
MABr	32 mg
FAI	240 mg
DMF	1088 uL
DMSO	272 uL
CsI	1 g
DMSO for CsI	2.566 mL

The mechanical process of fabricating the perovskite crystal requires multiple meticulous steps. The first step is to clean substrates utilizing the UV ozone cleaner For 15 minutes. Within 15 minutes of UV ozone cleaning, the perovskite film must be fabricated. The samples are spun coated in an inert environment. Using 110 uL of PSK solution, spin coat samples at 1000 RPM for 10 seconds, then 4000 RPM for 30 seconds. Ten seconds before the end of the spin, use a pipette to drop 150 uL of chlorobenzene (CBZ). Place samples immediately on hot plate set to 100° C to anneal for 30 minutes. Ideal perovskites should be black and have a moderate shine.

### Hole Transport Layer

The hole transport layer extracts holes from the perovskites and has a large impact on device performance. The fabrication of the hole transport layer involves a time sensitive chemical solution deposited with specific constraints. This chemical solution must be mixed in a precise order to achieve desired electrical properties.

In separate vials, weigh solid material for HTL. The weights listed in Table 2.1 must be as accurate as possible because variations in the amount of these materials cause undesirable variations in electrical performance. After solid materials are weighed, the solvents must be added to each respective vial. Mixing can be done by either handshaking each vial, or with a magnetic stirrer. No heat is required to properly dissolve solutions. Mix the respective solutions by first mixing 2,2',7,7'-Tetrakis[N,N-di(4-methoxyphenyl)amino]-9,9'-spirobifluorene Spiro-MeOTAD (Spiro-MeOTAD), 4tert-butylpyridine (4TBP), bis-(trifluoromethane)sulfonimide lithium salt (LiTFSI), and finally tris(2-(1Hpyrazol-1-yl)-4-tert-butylpyridine)cobalt(III)tris(bis-(trifluoromethane)sulfonimide) (FK209).

The end mixture should be a black or dark purple solution. This solution must be used immediately after mixing.

Table 2.1 HTM materials and weights

Material	Amount	Solvent	Amount	Amount of Solution needed for HTL
Spiro-OMeTAD	34.2 mg	CBZ	400 uL	400 uL
4TBP	11.2 uL	N/A	N/A	11.2 uL
LiTFSI	52 mg	(Acetonitrile) ACN	100 uL	6.8 uL
FK209	15 mg	ACN	100 uL	8.4 uL

To deposit the hole transport layer onto the perovskite, use a pipette to extract 50 uL of solution from the vial. The solution is deposited via spin coating in an inert environment. Samples are spun at 4000 RPM. Solution must be rapidly dropped 10 seconds before the completion of the spin. Once complete set aside sample on flat surface. All samples must be left in an inert and dark environment overnight so the lithium ions can dope the transport layer. It is critical that neither this layer nor the materials used to fabricate this layer be exposed to the outside air.

## Gold Electrodes

The metal electrodes are deposited via thermal evaporation. In an evaporator Bell jar, a gold wire is heated to evaporate gold particles onto the substrate. This final step completes the circuit of the solar cell.

Place samples in holder with stencil cutouts as seen in figure 12. From the gold wire measure 12 centimeters of gold and cut. Wrap gold wire around evaporator coil making good contact with the coil. This process is critical as it minimizes the time it takes to deposit gold and makes sure gold is deposited with regularity. Wash evaporator wrapped in gold wire within acetone rinse followed by an alcohol rinse. Once rinsed with alcohol blow coil with nitrogen gas to prevent film from forming. Wrap the evaporator coil in gold wire with aluminum foil to keep sanitary. Take each sample and scrape off all the preceding films from the ends of the sample perpendicular to resistive section of the sample. The exposed area should only be wide enough for one segment of the stencil and load the samples into the holder as seen in figure 12.

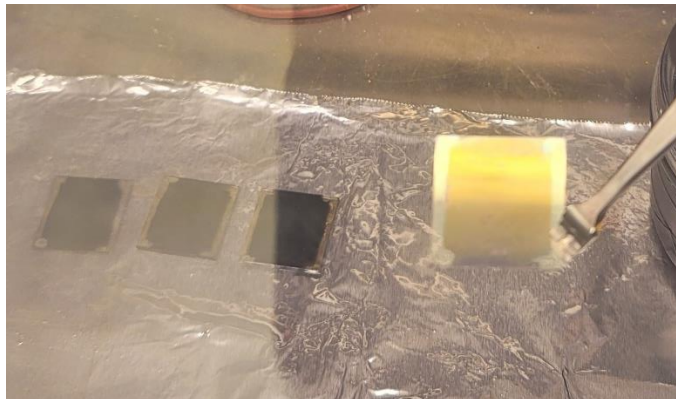


Figure 12 1: Correct removal of films for gold deposition.

Vent the thermal evaporator by first turning off the Turbo pump by pressing the stop button on the control panel. Once the pressure gauge reads any value on the scale of  $10^{-2}$  torrs open the vent on the side of the machine using the switch seen on the left side of the machine. Wait 60 seconds and turn off the mechanical pump. The typical time for bell jar to fully depressurize is 10 to 15 minutes. Once the bell can be easily lifted, load samples into machine stencil side down towards gold evaporator. Measure the distance between the gold wire and measurement crystal. Then measure the distance between the gold wire and the samples. Utilizing equation 13, calculate the tooling factor.

$$\text{Tooling Factor} = \left(\frac{D_C}{D_S}\right) * 100 \dots\dots\dots(13)$$

Wipe down the contact surfaces between the bell jar and the base to ensure a secure connection. Once this is done close the vent on the side of the machine and turn on the mechanical pump. Once the pressure gauge reads any value of scale  $10^{-2}$  torrs turn on the turbo pump. When the pressure gauge reads a value on the scale of  $10^{-5}$  torrs or below, begin gold deposition. Enable electrode contacts with the leftmost switch on the control panel. Turn on the switch for 220 volts. Slowly increase the voltage with the control nob until evaporator are coil starts to glow. The measurements instrumentation should be zeroed to ensure accuracy of results. The gold should be deposited at a rate of .5-1 angstroms per second (A/s). The final thickness of the gold layer should be 800 to 850 angstroms. The resulting samples should look like figure 13.

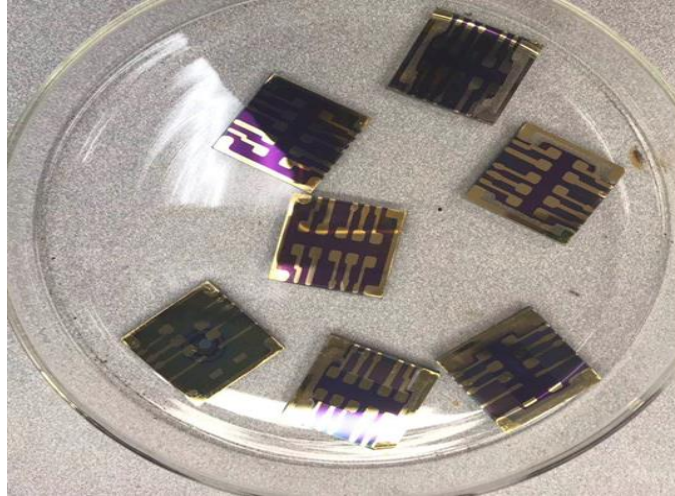


Figure 13 1: The fabricated perovskite solar cells after gold deposition.

### Results and Discussion

Perovskite solar cell research has shown much promise in recent years. Power conversion efficiencies have increased without fail. In this research effort, the results have confirmed the desirable properties of PSC. In figure 14, the PCE both the fabricated sample can be seen to be 13.58% with a fill factor of .61. the short circuit current density is 20.596 mA/cm<sup>2</sup> and the open circuit voltage is 1.03 V. These properties are how you desirable for use in solar energy. In figure 15, this fabricated sample has a PCE of 16.64 and a fill factor of .663. The short circuit current density is 22.69 mA/cm<sup>2</sup> and open circuit voltage of 1.106 V.



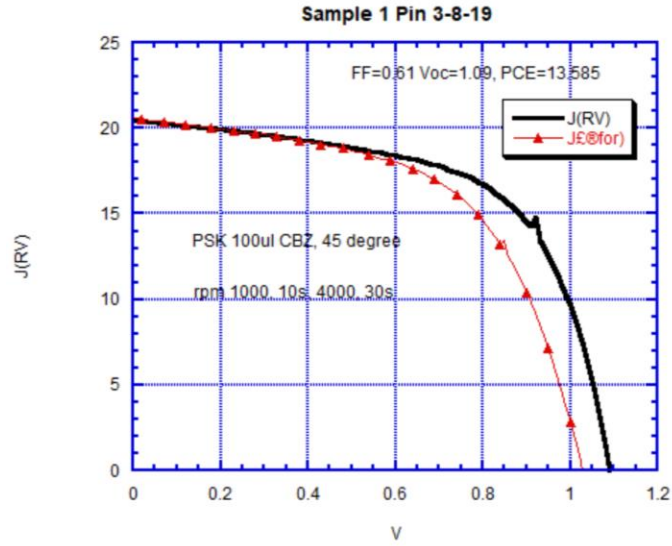


Figure 14 1: Current voltage relationship of Perovskite solar cell.

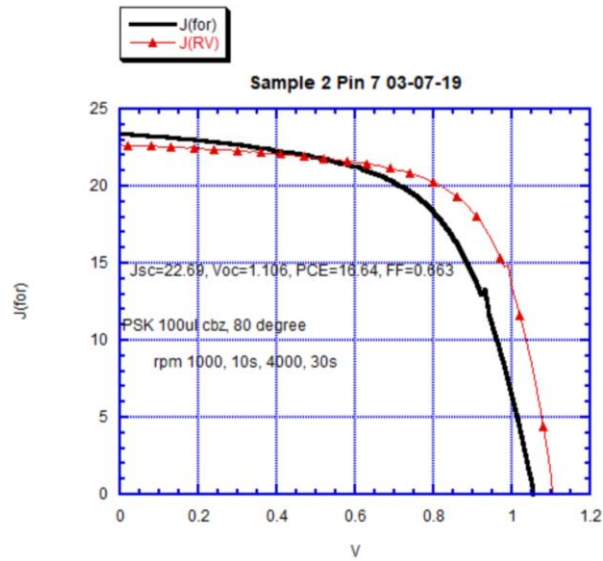


Figure 15 1: Current voltage relationship of Perovskite solar cell.

In figure 16, the PCE of the cell is 18.13% and the fill factor is .664. the short circuit current density is 24.689 and open circuit voltage of 1.11 V.

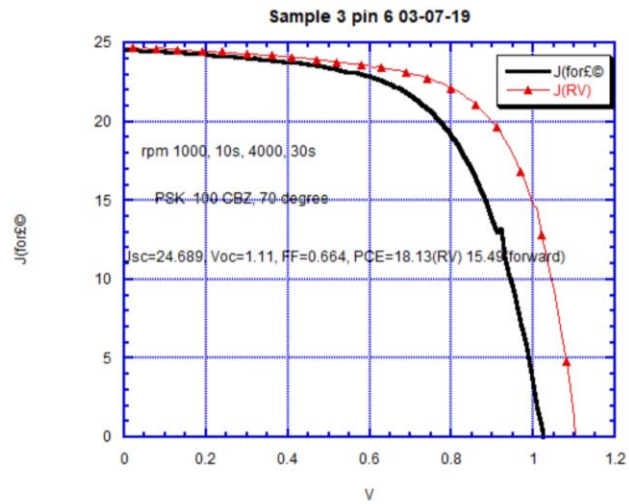


Figure 16 1: Current voltage relationship of Perovskite solar cell.

The PSC current voltage curve of figure 17 has a PCE of 15.97% and a fill factor of .65.

The open circuit voltage is 1.11V and the short circuit current density is 22.18 mA/cm<sup>2</sup>.

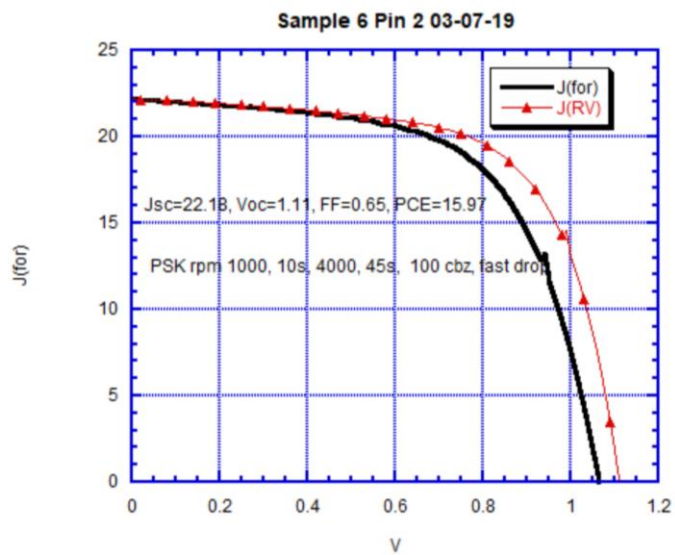


Figure 17 1: Current voltage relationship of Perovskite solar cell.

## CHAPTER 4. DATA COLLECTION METHODOLOGY

### 4.1 Data Acquisition and Analysis

While scientific research is heavily dependent on the following of experimental procedures, this process will be completely moot without proper data acquisition and analysis. The use of scientifically accurate measuring instruments ensures that the results collected are accurate and precise. In this research effort, the data collection is based on emulating environmental conditions in which fabricated solar cells would operation. Fabricated PCEs are measured for their current voltage relationship, fill factor, and device behavior in the dark. This data indicates the intricate quantum mechanics within the device and their relationship to the preceding chemistry.

While fabricated samples offer invaluable information, there are other means of data acquisition for PSC research. Utilizing a virtual environment PSCs can be simulated and experimented with. We look at several configurations and simulation techniques in order to further research be physics of PSCs. In these simulations, viability and application is demonstrated for PSC research. This powerful tool allows research to be conducted which fabrication labs currently are unable to perform. The results yielded from these computer-generated simulations offers invaluable insight and contributes to the breadth of knowledge about PSC. Thereby further legitimizing this research effort.

### 4.2 Fabricated Sample Testing

Testing the electronic properties of PSCs is critical to the progression of PSC research. Given standard operating conditions such as irradiance and temperature, the

samples are tested to see their electrical response. How efficiently the fabricated samples convert optical power into electrical power directs ongoing research. These results can indicate experimental errors, human errors, mechanical issues, and can possibly terminate research. In this section the procedure for collecting data of our paid devices is outlined.

The fabricated samples should be kept in a light tight container. Transfer the container with the samples into an inert glove box with the testing setup as seen in figure 18.

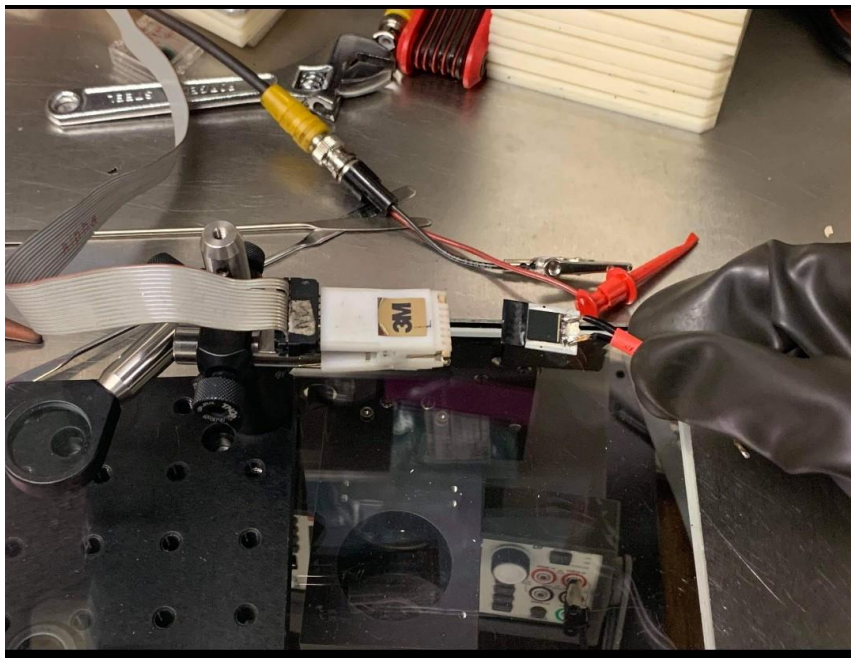


Figure 18 1: Solar Simulator Setup with multimeter.

Turn on the back then front switches of the solar simulator as seen in figure 19.1 in 19.2.



Figure 19 1: Back Power switch of Solar Simulator.

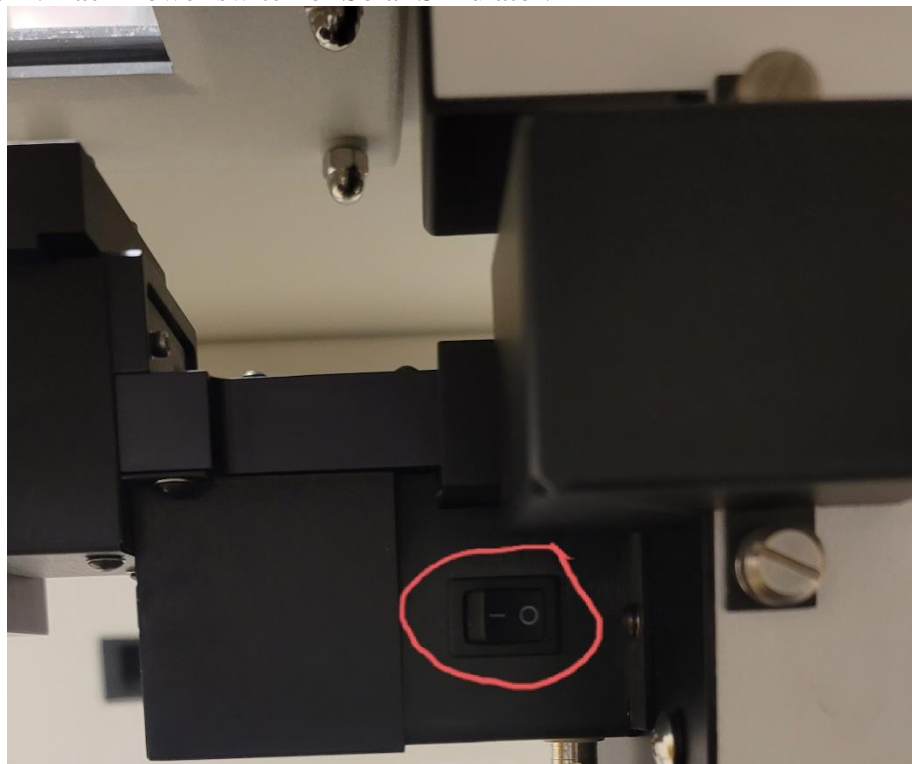


Figure 19 2: Front Power switch of Solar Simulator.

Position the testing stand to the edge of the illuminated area. Using the multimeter with the irradiance detector, find the height which yields  $1000 \text{ W/m}^2$ . position the stands to match this height of the meter. Remove a sample from the light tech container and match the gold electrodes to the pin of the holder. Take note of the pins which coincide with the electrodes. While not all electrodes will sufficiently coincide with deposited goals, ensure that the electrodes deposited on the FTO (ITO) match the pin of the holder. using the turning nob switch outside of the glove box, adjust the switch to match the pins which are aligned with the electrodes. With the control computer outside of the glove box as seen in figure 16, run a scan of the device at different voltages. Forward scan is when the voltage is incrementally increasing. Reverse scan is when the voltage is incrementally decreasing. reverse scans should be done first followed by forward scans for pins which have be best results. If one chooses to, forward and reverse scans can be performed for each pin. After turning off the solar simulator cover the device with your hands without touching the sample. Run a reverse scan to find the diode curve. this scan shows the threshold voltage of the PSC as a semiconductor. Without the light generated current, the diode current can be assessed. Following each scan save collected data in the format of whether scan was under lights or dark, the sample number or letter, which pin is being tested, and whether the scan was forward or reverse. For example, if sample 2 on pin 3 was tested under illumination in reverse scan the file format would be "2-3-light-rev.txt". This formatting is critical to the organization of the data. Without proper formatting and organization of data collected errors are highly likely to occur. Once this data is collected analysis and graphing must be done in order to draw accurate conclusions.

Using data processing tools such as Kaleida Graph, Labview, and Microsoft Excel software, data is analyzed for qualities such as fill factor, maximum power point, and hysteresis. To plot the current voltage relationship, physics must be considered. To the measurement equipment, the current is negative because of the direction in which it is flowing with respect to the applied voltage. However, this must be corrected as it skews analysis. Considering the absolute value of the photogenerated current is more representative of the magnitude of PCE. The sampling time of the equipment produces a discrete set of points for the graphing software to analyze. This discrete  $N \times 3$  matrix can be adjusted by adjusting the sampling time. This small degree of variance in accuracy is immaterial to the conclusions drawn.

After loading data files onto a computer and downloading KaleidaGraph software, unzip the software package. Open the file named Kaleida.exe. In this software, select the file which you are trying to graph. Select the delimiter as "tab" and set the number to  $\geq 1$ . This ensures the data is parsed correctly. In column A, the current is displayed. Select the column and copy it to your clipboard. Open Microsoft Excel and paste the data in one of the columns utilizing another column, write the formula for the column you selected multiplied by negative one. Copy this column, and paste it within the area of the original data. Once the data populates in a data table as seen in figure 20, select the Gallery tab, linear, then select line.

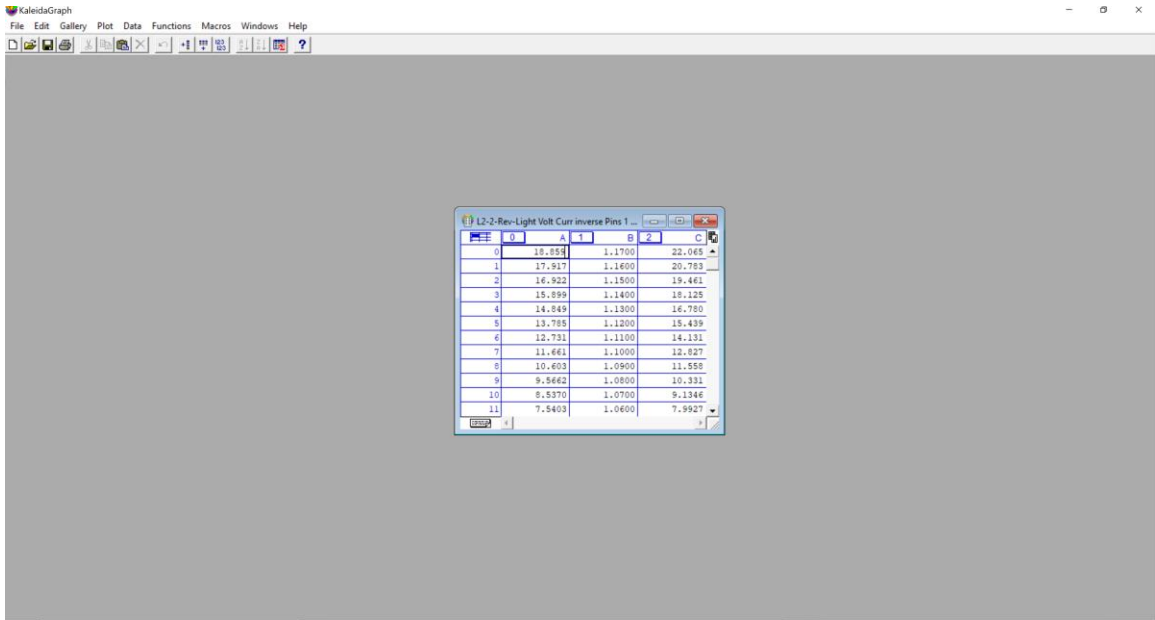


Figure 20 1: KaleidaGraph screen after data is populated.

In the data table column C represents the power at each point. The maximum power point can be easily seen from the highest value of the set.



## CHAPTER 5. SIMULATION OF PEROVSKITE SOLAR CELLS

### 5.1 Perovskite Solar Cell Simulation

Simulating a PSC is heavily reliant on knowing the unique semiconductor characteristics of the PSC. By varying the intrinsic properties of the simulated solar cell, a PSC can be experimented with in a virtual environment [44]. This powerful tool allows inner device parameters such as negative capacitance and interlayer physics to be explored. The flexibility of device modeling allows different materials and configurations to be explored. This method was implemented in order to create the simulated cell seen in figure 21.

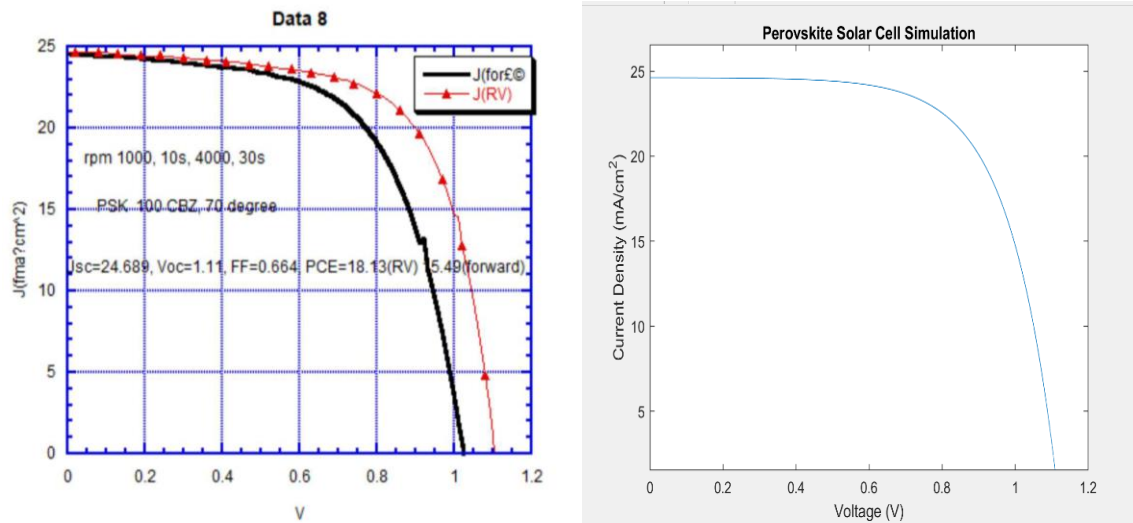


Figure 21 1: Current voltage curve of fabricated cell and simulated PSC.

In SIMULINK, the characteristics of the solar cell are manipulated to match that of a PSC. utilizing this simulated circuit the current voltage relationship was modeled based on a fabricated sample which had a high PCE. these results signify that a PSC can be created virtually. Given this result, simulated results were expanded in their analysis.

Based on the data, analyzing perovskite solar cells based on ideality factor is a viable and reliable tool for perovskite solar cell development. The fabricated samples were tested in an inert environment for their current voltage relationship. This data is plotted using Kaleida graphing software. The ideality factor is calculated by taking the data for the samples and processing it via a MATLAB script. The graphs show the voltage current relationship of a fabricated  $\text{Cs}_{0.05}(\text{MA}_{0.15}\text{FA}_{0.85})_{0.95}\text{Pb}(\text{I}_{0.85}\text{Br}_{0.15})_3$  perovskite cell and its ideality factor. Given the ideality factor of the fabricated solar cells is greater than 2, the dominate recombination process in this cell seems to be higher order trap assisted recombination at the interface of the perovskite and the transport layers. Figure 22 illustrates the current voltage relationship of a fabricated perovskite solar cell and its simulated counterpart. The low hysteresis between the forward ( $J(\text{for})$ ) and reverse ( $J(\text{RV})$ ) scans, high short circuit current, and high open circuit voltage are all desirable characteristics of these devices. This indicates the crystallization process produced perovskite nanocrystals that are larger and more homogeneous [46]. The high-power conversion efficiency shows good charge transport and reduced non-radiative loss at the interfacial layers of the device. Figure 23 shows similar behavior with slightly more hysteresis and the simulated cell. Both devices have a small deviation from this behavior between 0.8 and 1 volt. This could be due to a defect in the device or an irregularity in the perovskite crystal itself. The ideality factor of the solar cell of figure 22 is found to be 2.32. In figure 23 the ideality factor of the cell was found to be 2.27. given the ideality factor is approximately 2 in both samples, the dominant recombination mechanism can be determined to be trap assisted states of a at least one mid bandgap state. The number of intermediate sites cannot be quantified simply from the ideality factor as third or fourth order recombination at various rates can produce this

ideality factor. The trap assisted recombination has a midgap energy level trap for recombination. This deep trap recombination can either have high current densities in the bulk of the perovskite or at the interfacial layers. However, what is evident from these derived ideality factors that the charge densities of the holes and the electrons are approximately equal in the crystal [47]. These values are above the known ideality factor for SRH recombination indicating the possibility of nonlinear shunt resistance or large gradients in recombination current densities. Following the theory of mid-gap assisted recombination, recombination takes place in the depletion region of the cell. In an ideal, only direct recombination outside of the depletion region occurs. Due to the shunt resistance, capacitive properties, and recombination in the depletion region of organic electronics, the ideality factor is above 2 and influences direct band-to-band recombination [48]. Utilizing simulation and modeling techniques, the intellectual merits and scientific contribution of simulated PSCs has been demonstrated in this research work. In figure 24, the current voltage relationship of a PSC with a 2 nm silver intermediate layer between the gold and HTL is shown and its corresponding simulated cell. A silver interlayer has shown to enhance the bonding of the gold electrode as seen in figure 25. Given the legitimacy of this practice, it would stand to reason to explore possible applications and engineering design schemes for this technology. Given the inflation of demands and problems in power engineering it stands to reason that PSC may be applicable in a smart grid.

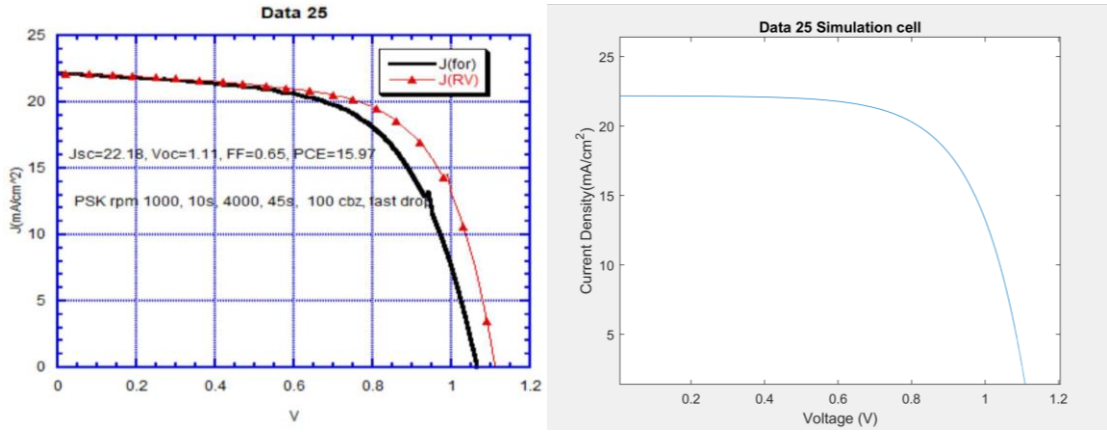


Figure 22 1: Current voltage relationship of fabricated perovskite cell.

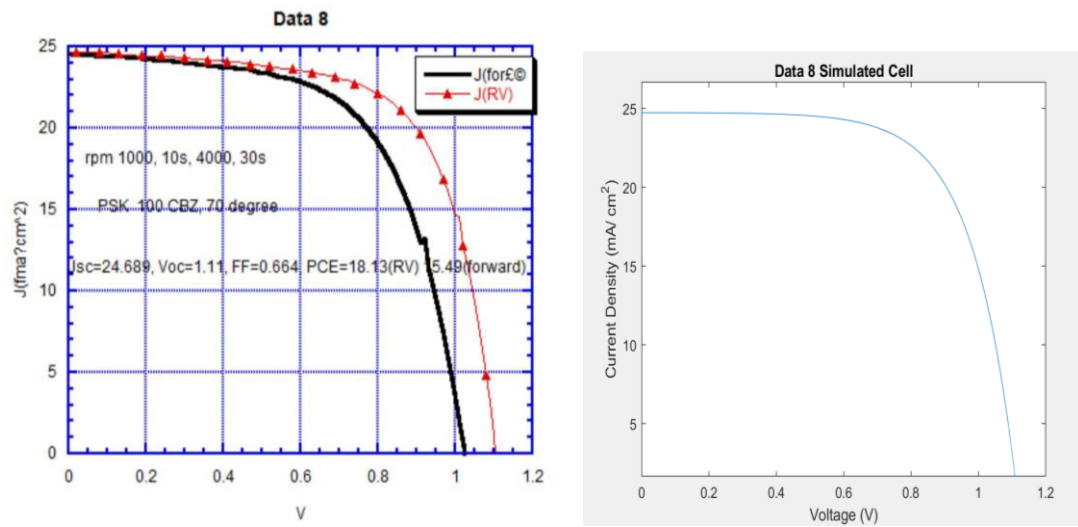


Figure 23 1: Current voltage relationship of fabricated perovskite cell.

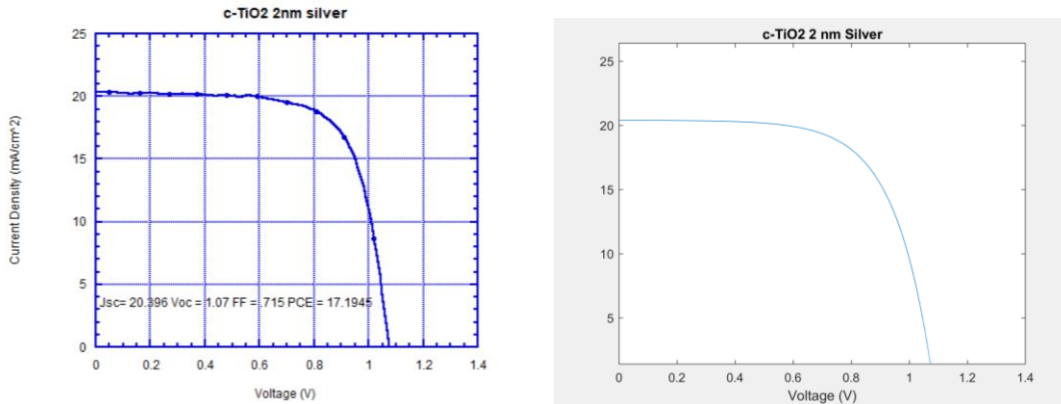


Figure 24 1: PSC with 2 nm of silver deposited and its corresponding simulated cell.

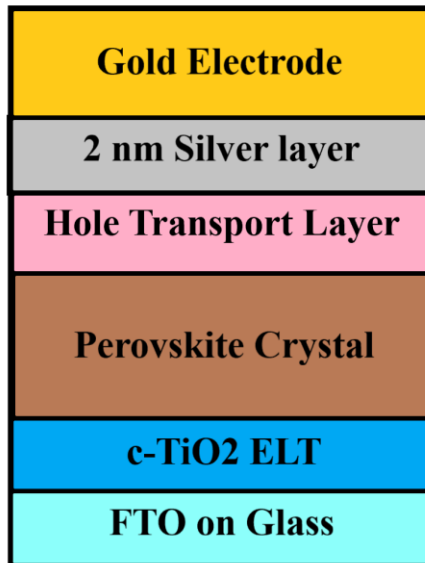


Figure 25 1: Layer construction of PSC with 2 nm Silver layer.

High efficiency perovskites have the potential to become a leading material for third generation photovoltaics. With emerging trends in energy production favoring solar energy, perovskites could be a viable option for solar smart grid construction. In this work, perovskites were utilized in a residential smart grid simulated in SIMULINK. Our results

demonstrate the viability of perovskite solar panels is demonstrated. The simulation was based on fabricated mixed cation solar cells. These simulated cells have been shown to be an accurate and valuable tool in Perovskite solar cell research [44]. By manually configuring the parameters of the solar cell, a photovoltaic array of perovskite solar panels was simulated. Parameters such as light generated current, diode saturation current, and diode ideality factor analyzed from a fabricated cell [45]. This simulated perovskite photovoltaic array was compared to a commercially available A10J-S72-175 solar panel by A10 Green Technology. The arrays had the characteristics seen in table 3.1.

Table 3.1 Simulation of a Solar Module with PSK and Commercial Solar Module

<b>Characteristics</b>	<b>Solar Module</b>	
	<b>Solar module with 72 Perovskite cells</b>	<b>Commercial A10J-S72-175 solar module with 72 cells</b>
<b>Open Circuit Voltage</b>	<b>79.92 V</b>	<b>43.99 V</b>
<b>Short Circuit Current</b>	<b>6.008 A</b>	<b>5.17 A</b>
<b>Light Generated Current</b>	<b>6.008 A</b>	<b>5.178 A</b>
<b>Diode Ideality Factor</b>	<b>2.27</b>	<b>.98852</b>
<b>Power Conversion Efficiency</b>	<b>18.13 %</b>	<b>17 %</b>
<b>Diode Saturation Current</b>	<b>.1 nA</b>	<b>.1784 nA</b>

The PV arrays were attached to a smart grid and the measured for their performance. We can see the Perovskite PV array performed well compared to commercially available solar panels. The power output of the PV arrays can be seen in Figure 26.

Table 3.2 Simulation of a Solar Module with our cells and a commercial Module

Configuration Parameters	Our Perovskite	A10J-S72-175 solar panel
Number of cells per module	72	72
Fill factor	.664	.74
Parallel module strings	4	4
Modules in series	10	10

### SIMULINK Simulation of Smart Grid

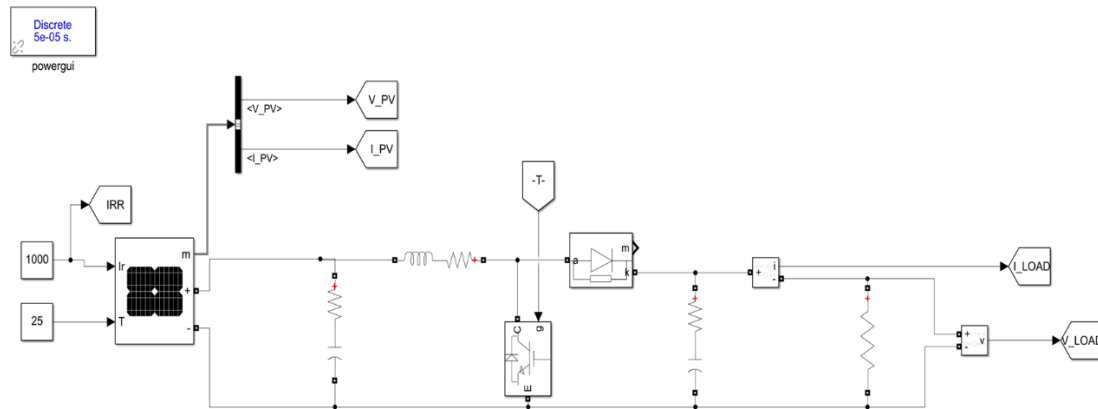


Figure 26: The power Output of a PSC smart grid vs smart grid with commercial solar panels.

From this figure, we can see the perovskite solar panel has high transient stability and low settling time. The perovskite produced 7.6 kW and the commercial panels produced 6.8 kW.





## CHAPTER 6. CONCLUSION AND FUTURE WORK

### 6.1 Conclusion

While the future is always ambiguous, the energy demands of today and technological advances makes it clear that solar energy is the method of energy production of the future. The need for energy that is environmentally conscious and sustainable has never been more apparent. With the challenges that current solar panel technology present, there is a need for a new generation of photovoltaic materials. These materials must be highly efficient at converting optical energy into electrical energy. Because of the economics of engineering, this technology also must be less than or equal to the current methods of fossil fuel energy production. With perovskite solar cells, this goal can be met. Utilizing the simulation in fabrication of PSCs, PSKs can be experimented with to test their optical, electrical, and quantum characteristics. Simulated PSCs have been shown to be scientifically accurate and produces meaningful results. Utilizing simulated PSCs, applications and configurations based on this PV technology can be experimented with. this virtual experimentation surpasses the limits of fabrication labs. In a virtual setting PSCs have been shown to be effective in a smart grid topology. The semiconductor properties of PSCs can be ascertained via computational means in order to connect the electrical properties, the internal quantum mechanics, and the preceding chemistry. Given these results, fabrication research can be directed in order to enhanced desirable characteristics and address issues for being this technology from commercial use. Current methods such as anion and cation excessing, open circuit voltage enhancements, and

lowering concentration of defects has shown to be effective at enhancing the PCE of PSCs. utilizing these techniques to fabricate a PSC simulation, machine learning, and computational analysis can shed lights on how these methods affect the intrinsic properties of the crystal. These simulation techniques have the advantage of lowering the cost of PSC experimentation. By lowering the costs of experimenting with this technology, the population of researchers working in this area becomes maximized. The results show that PSC based systems are viable. This result is significant because fabricating a PSK solar panel array is not currently possible. Production techniques, architecture, and logistical barriers forebay implementation of this technology in a smart grid topology at this point. Therefore demonstrating and in virtual environment that PSC can be used in power engineering in a scalable fashion offers a significant contribution to the field of science. given this viability in application, future work can pursue this end when research methods allow it.

## 6.2 Future Work

PSC research has overcome many challenges. The power conversion efficiency of PSCs has increased faster than many proceeding PV technologies that came before it. While this incredible advance cannot be underestimated, much work is needed in order to realize commercially available PSC. In order to proliferate low cost solar energy, perovskites must be produced on a commercial scale. Many factors play into the crystallization of perovskite. One of the most critical parameters is the impact water has on performance. Currently, PSKs must be fabricated in an inert environment with no more than 5 PPM of water in the air and no more than 10 PPM of oxygen in the air. This presents a significant challenge for manufacturing and production. PSCs Which can be fabricated

in ambient conditions must be developed to make commercial production feasible. The transport layers within a PSC can vary depending on the architecture and the substrate. Titanium oxide requires an annealing temperature of 400 C. Conversely, tin oxide requires an annealing temperature of 65 C. Therefore, tin oxide is a more ideal ETL for flexible substrates. Roll to roll manufacturing can be realized with further development PSC with a SnO<sub>2</sub> ELT. The physical characteristics of the perovskite has shown variance with different fabrication techniques. Manufacturing scale fabrication such as printing, slot die coating, and spray paralysis yield vastly different PCEs. Developing a manufacturing technique for PSK fabrication is critical to the proliferation of PSC technology. Researching the chemistry of PSCs is needed to identify ideal combinations and maximize PCE. Mixed cation and mixed anion PSKs have shown increased PCEs in a laboratory setting. Further research is required to understand the quantum mechanics and electrical phenomenon happening within the PSK crystal to make this so. Optimization is a necessary process to fully realize the full potential of any PSC because non ideal ratios of precursor chemicals cause lower PCE. Many data points would be required in order to realize optimization of a PSK. Varying the ratio of cations as well as anions shows how the chemistry of affects the electrical properties. With this data, trends and formula can be derived in order to subsequently develop different types of PSK for use in PSC. Varying the amounts of additives also identifies optimal points in PSC. The addition of inorganic salts changes the morphology of the PSK crystal. How and why this variance occurs is critical to optimal concentrations of additives. Material properties such as atomic radii and Electronegativity play a critical role in the optical and electrical properties of PSK. It is currently not known how the lattice constants of a crystal affects its bandgap. One of the

most beneficial qualities of PSKs is the ease with which their bandgap can be varied, the relationship between lattice constants and optical properties can be discovered. This future work stands to increase our understanding of optoelectronics, nano technology, and simultaneously disseminate renewable energy.

## BIBLIOGRAPHY

- [1] T. Jenkins, "A brief history of ... semiconductors," *Physics Education*, vol. 40, no. 5, pp. 430–439, 2005.
- [2] S. Dimitrijević, *Principles of semiconductor devices*, 2nd ed. New York: Oxford University Press, 2012.
- [3] H. H.-T. Corporation., "4. History of semiconductors," *4. History of semiconductors : Hitachi High-Tech GLOBAL*. [Online]. Available: <https://www.hitachi-hightech.com/global/products/device/semiconductor/history.html>. [Accessed: 25-Mar-2021].
- [4] E. Chu and L. Tarazano, "A Brief History of Solar Panels," *Smithsonian.com*, 22-Apr-2019. [Online]. Available: <https://www.smithsonianmag.com/sponsored/brief-history-solar-panels-180972006/>. [Accessed: 30-Mar-2021].
- [5] "How a Solar Cell Works," *American Chemical Society*. [Online]. Available: <https://www.acs.org/content/acs/en/education/resources/highschool/chemmatters/past-issues/archive-2013-2014/how-a-solar-cell-works.html>. [Accessed: 10-Apr-2021].
- [6] J. C. Lee, S. W. Jun, J. H. Yun, S. K. Kim, J. Song, and K. H. Yoon, "Si-based thin-film solar cells: process and device performance analysis," *Conference Record of the Thirty-first IEEE Photovoltaic Specialists Conference*, 2005.
- [7] M. T. Kibria, A. Ahammed, S. Sonny, F. Sony, and S.-U.-I. Hossain, "A Review: Comparative studies on different generation solar cells technology," *Conference: 5th International Conference on Environmental Aspects of Bangladesh [ICEAB 2015]*, Sep. 2014.
- [8] H. A. Mohamed, "Dependence of efficiency of thin-film CdS/CdTe solar cell on optical and recombination losses," *Journal of Applied Physics*, vol. 113, no. 9, p. 093105, 2013.
- [9] T. J. van der Werff, "Greatest engineering achievements of the 20th century," National Academy of Engineering, Washington, DC, Dec. 2000.
- [10] "U.S. Energy Information Administration - EIA - Independent Statistics and Analysis," *U.S. energy facts explained - consumption and production - U.S. Energy Information Administration (EIA)*, 07-May-2020. [Online]. Available: <https://www.eia.gov/energyexplained/us-energy-facts/>. [Accessed: 10-Apr-2021].

- [11] T. J. van der Werff, BGreatest engineering achievements of the 20th century, National Academy of Engineering, Washington, DC, Dec. 2000.
- [12] “The Modern Grid Strategy,” Jun-2009. [Online]. Available: [https://netl.doe.gov/sites/default/files/Smartgrid/Whitepaper\\_The-Modern-Grid-Vision\\_APPROVED\\_2009\\_06\\_18.pdf](https://netl.doe.gov/sites/default/files/Smartgrid/Whitepaper_The-Modern-Grid-Vision_APPROVED_2009_06_18.pdf). [Accessed: 01-Feb-2021].
- [13] National Energy Technology Laboratory (2009). *A Vision for a Smart Grid*. [online] Department of Energy. Available at: [https://www.netl.doe.gov/sites/default/files/Smartgrid/Whitepaper\\_The-Modern-Grid-Vision\\_APPROVED\\_2009\\_06\\_18.pdf](https://www.netl.doe.gov/sites/default/files/Smartgrid/Whitepaper_The-Modern-Grid-Vision_APPROVED_2009_06_18.pdf) [Accessed 5 Feb. 2020].
- [14] Taft, J. and Martini, P. (2016). *Sensing and Measurement Architecture for Grid Modernization*. [ebook] Pacific Northwest National Laboratory, p.4. Available at: <https://gridarchitecture.pnnl.gov/media/advanced/Sensor%20Networks%20for%20Electric%20Power%20Systems.pdf> [Accessed 5 Feb. 2020].
- [15] B. C. C. R. Editorial, *A History of Perovskite Solar Cells*, 06-Mar-2018. [Online]. Available: <https://blog.bccresearch.com/a-history-of-perovskite-solar-cells>. [Accessed: 03-Apr-2021].
- [16] “Best Research-Cell Efficiency Chart,” *NREL.gov*. [Online]. Available: <https://www.nrel.gov/pv/cell-efficiency.html>. [Accessed: 04-Apr-2021].
- [17] Q. Lin, A. Armin, P. L. Burn, and P. Meredith, “Organohalide Perovskites for Solar Energy Conversion,” *Accounts of Chemical Research*, vol. 49, no. 3, pp. 545–553, Oct. 2015.
- [18] Saliba, Michael & Correa-Baena, Juan-Pablo & Wolff, Christian & Stollerfoht, Martin & Phung, Nga & Albrecht, Steve & Neher, Dieter & Abate, Antonio. (2018). How to Make over 20% Efficient Perovskite Solar Cells in Regular (n–i–p) and Inverted (p–i–n) Architectures. *Chemistry of Materials*. 30. 10.1021/acs.chemmater.8b00136.
- [19] Saliba, Michael & Matsui, Taisuke & Domanski, Konrad & Seo, Ji-Youn & Ummadisingu, Amita & Zakeeruddin, Shaik & Correa-Baena, Juan-Pablo & Tress, Wolfgang & Abate, Antonio & Hagfeldt, Anders & Graetzel, Michael. (2016). Incorporation of rubidium cations into perovskite solar cells improves photovoltaic performance. *Science (New York, N.Y.)*. 354. 10.1126/science.aah5557.
- [20] C. A. Otálora, G. Gordillo, L. Herrera, and J. Estrada, “Effect of the solution chemistry on the film growth of hybrid MAPbI<sub>3</sub> perovskites,” *Journal of Materials Science: Materials in Electronics*, vol. 32, no. 6, pp. 6912–6918, Feb. 2021.
- [21] Huang, Fei & Li, Mengjie & Siffalovic, Peter & Cao, Guozhong & Tian, Jianjun. (2019). From scalable solution fabrication of perovskite films towards commercialization of solar cells. *Energy & Environmental Science*. 12. 10.1039/C8EE03025A.

- [22] Jiang Q, Zhang X, You J. SnO<sub>2</sub> : A Wonderful Electron Transport Layer for Perovskite Solar Cells. *Small* (Weinheim an der Bergstrasse, Germany). 2018 Jun:e1801154. DOI: 10.1002/sml.201801154.
- [23] M. Ding, L. Sun, X. Chen, T. Luo, T. Ye, C. Zhao, W. Zhang, and H. Chang, “Air-processed, large grain perovskite films with low trap density from perovskite crystal engineering for high-performance perovskite solar cells with improved ambient stability,” *Journal of Materials Science*, vol. 54, no. 18, pp. 12000–12011, Jun. 2019.
- [24] Jiang, Qi & Chu, Zema & Wang, Pengyang & Yang, Xiaolei & Liu, Heng & Wang, Ye & Yin, Zhigang & Wu, Jinliang & Zhang, Xingwang & You, Jingbi. (2017). Planar-Structure Perovskite Solar Cells with Efficiency beyond 21%. *Advanced Materials*. 29. 10.1002/adma.201703852.
- [25] J. Yang, S. Chen, J. Xu, Q. Zhang, H. Liu, Z. Liu, and M. Yuan, “A Review on Improving the Quality of Perovskite Films in Perovskite Solar Cells via the Weak Forces Induced by Additives,” *Applied Sciences*, vol. 9, no. 20, Oct. 2019.
- [26] S. Agarwal and P. R. Nair, “Pinhole induced efficiency variation in perovskite solar cells,” *Journal of Applied Physics*, vol. 122, no. 16, 2017.
- [27] M. Pandey, G. Kapil, K. Sakamoto, D. Hirotani, M. A. Kamrudin, Z. Wang, K. Hamada, D. Nomura, H.-G. Kang, H. Nagayoshi, M. Nakamura, M. Hayashi, T. Nomura, and S. Hayase, “Efficient, hysteresis free, inverted planar flexible perovskite solar cells via perovskite engineering and stability in cylindrical encapsulation,” *Sustainable Energy & Fuels*, vol. 3, no. 7, 2019.
- [28] W. A. Saidi, W. Shadid, and I. E. Castelli, “Machine-learning structural and electronic properties of metal halide perovskites using a hierarchical convolutional neural network,” *npj Computational Materials*, vol. 6, no. 1, 2020.
- [29] H. Bellia, R. Youcef, and M. Fatima, “A detailed modeling of photovoltaic module using MATLAB,” *NRIAG Journal of Astronomy and Geophysics*, vol. 3, no. 1, pp. 53–61, 2014.
- [30] J. Li, B. Pradhan, S. Gaur, and J. Thomas, “Perovskite Solar Cells: Predictions and Strategies Learned from Machine Learning to Develop High-Performing Perovskite Solar Cells (Adv. Energy Mater. 46/2019),” *Advanced Energy Materials*, vol. 9, no. 46, p. 1970181, 2019.
- [31] Q. Xu, Z. Li, M. Liu, and W.-J. Yin, “Rationalizing Perovskite Data for Machine Learning and Materials Design,” *The Journal of Physical Chemistry Letters*, vol. 9, no. 24, pp. 6948–6954, 2018.
- [32] Cheknane, A., Hilal, H., Djeflal, F., Benyoucef, B. and Charles, J., 2008. An equivalent circuit approach to organic solar cell modelling. *Microelectronics Journal*, 39(10), pp.1173-1180.

- [33] M. Taghavi, M. Houshmand, M. Zandi and N. Gorji, "Modeling of optical losses in perovskite solar cells", *Superlattices and Microstructures*, vol. 97, pp. 424-428, 2016. Available: 10.1016/j.spmi.2016.06.031.
- [34] Z. Liu, J. Chen, C. Huang, T. G. Kiprono, W. Zhao, W. Qiu, Z. Peng, and J. Chen, "Dependence of Precursors on Solution-Processed SnO<sub>2</sub> as Electron Transport Layers for CsPbBr<sub>3</sub> Perovskite Solar Cells," *Nano*, vol. 15, no. 12, Nov. 2020.
- [35] Han, Li & Gao, Yan & Guo, Ying & Gao, Xing & He, Wen. (2020). Progress in Preparation of Electron Transport Layer in Perovskite Solar Cell. *Key Engineering Materials*. 861. 295-300. 10.4028/www.scientific.net/KEM.861.295.
- [36] "Best Research-Cell Efficiency Chart," *NREL.gov*, 22-Sep-2020. [Online]. Available: <https://www.nrel.gov/pv/cell-efficiency.html>. [Accessed: 13-Dec-2020].
- [37] P. Chen, Y. Bai, and L. Wang, "Minimizing Voltage Losses in Perovskite Solar Cells," *Small Structures*, Oct. 2020.
- [38] M. Saliba, T. Matsui, J.-Y. Seo, K. Domanski, J.-P. Correa-Baena, M. K. Nazeeruddin, S. M. Zakeeruddin, W. Tress, A. Abate, A. Hagfeldt, and M. Grätzel, "Cesium-containing triple cation perovskite solar cells: improved stability, reproducibility and high efficiency," *Energy & Environmental Science*, vol. 9, no. 6, pp. 1853–2160, Mar. 2016.
- [39] Y. Liu, B. J. Kim, H. Wu, L. Yuan, H. Zhu, A. Liu, and E. M. J. Johansson, "Flexible Lead Bromide Perovskite Solar Cells," *ACS Applied Energy Materials*, Sep. 2020.
- [40] M. Saliba, J.-P. Correa-Baena, C. M. Wolff, M. Stollerfoht, N. Phung, S. Albrecht, D. Neher, and A. Abate, "How to Make over 20% Efficient Perovskite Solar Cells in Regular (n-i-p) and Inverted (p-i-n) Architectures," *Chemistry of Materials*, vol. 30, no. 13, pp. 4193–4201, 2018.
- [41] S. Naqvi and A. Patra, "Hole transport materials for perovskite solar cells: A computational study," *Materials Chemistry and Physics*, vol. 258, Sep. 2020.
- [42] Asare, J. & Sanni, Dahiru & Agyei-Tuffour, Benjamin & Ernest, Agede & Oyewole, Oluwaseun & Yerramilli, Aditya & Doumon, Nutifafa. (2021). A Hybrid Hole Transport Layer for Perovskite-Based Solar Cells. *Energies*. 14. 1949. 10.3390/en14071949.
- [43] Lin, Yin-Sheng & Li, Hsin & Yu, Wen-Sheng & Wang, Szu-Tan & Chang, Yi-Min & Liu, Tsung-Hsin & Li, Shao-Sian & Watanabe, Motonori & Chiu, Hsiao-Han & Wang, Di-Yan & Chang, Yuan. (2021). [2.2]Paracyclophane-based hole-transporting materials for perovskite solar cells. *Journal of Power Sources*. 491. 229543. 10.1016/j.jpowsour.2021.229543.



- [44] M. Workman, D. Z. Chen and S. M. Musa, "Csx MA<sub>1-x</sub> Pb(I<sub>1-x</sub> Br<sub>x</sub>)<sub>3</sub> Perovskite Solar Cell Fabrication and Modeling," 2020 International Conference on Technology and Policy in Energy and Electric Power (ICT-PEP), Bandung, Indonesia, 2020, pp. 116-120, doi: 10.1109/ICT-PEP50916.2020.9249794.
- [45] M. Workman, S. Musa, and Z. Chen, "Ideality Factor Based Computational Analysis of Perovskite Solar Cells," 2021 IEEE Conference on Technologies for Sustainability, 2021
- [46] M. Ding et al., "Air-processed, large grain perovskite films with low trap density from perovskite crystal engineering for high-performance perovskite solar cells with improved ambient stability", *Journal of Materials Science*, vol. 54, no. 18, pp. 12000-12011, 2019. Available: 10.1007/s10853-019-03768-2.
- [47] P. Calado, D. Burkitt, J. Yao, J. Troughton, T. M. Watson, M. J. Carnie, A. M. Telford, B. C. O'Regan, J. Nelson, and P. R. Barnes, "Identifying Dominant Recombination Mechanisms in Perovskite Solar Cells by Measuring the Transient Ideality Factor," *Physical Review Applied*, vol. 11, no. 4, 2019.
- [48] O. Almora, K. T. Cho, S. Aghazada, I. Zimmermann, G. J. Matt, C. J. Brabec, M. K. Nazeeruddin, and G. Garcia-Belmonte, "Discerning recombination mechanisms and ideality factors through impedance analysis of high-efficiency perovskite solar cells," *Nano Energy*, vol. 48, pp. 63–72, 2018.

## MANIELL WORKMAN VITA

### Educational Institutions Attended

Bachelor of Science: Electronics Engineering  
Vaughn College Of Aeronautics And Technology May 2016  
GPA: 3.56 / 4.0, Cum Laude)

### Professional Positions Held

RCM Technology: International Trade Engineer

### Scholastic Honors

Cum Laude 2016

### **Publications:**

Maniell Workman, Zhi David Chen and Sarhan Musa, "Perovskite Solar Cell Simulation Using Modeling Software", ECS (PRiME) Meeting Abstract, vol. MA2020-02, 2632, (Oct. 4 - Oct. 9, 2020).

Maniell Workman, Hojjatollah Sarvari, So Min Park, Douglas R. Strachan, Kenneth Graham, Vijay P. Singh, and Zhi David Chen, "Mixed Halide perovskite for High-Quality Perovskite Solar Cells", 236th ECS Meeting, Atlanta, Georgia, Oct. 13-17, 2019.

Maniell Workman; David Zhi Chen; Sarhan M. Musa, Cs<sub>x</sub>MA<sub>1-x</sub>Pb(I<sub>1-x</sub>Br<sub>x</sub>)<sub>3</sub> Perovskite Solar Cell Fabrication and Modeling, 2020 International Confernece of Technology and Policy in Energy and Electric Powe, Bandung, Indonesia(2020); <https://ieeexplore.ieee.org/document/9249794>

Maniell Workman; David Zhi Chen; Sarhan M. Musa, "Machine Learning for Predicting Perovskite Solar Cell Opto-Electronic Properties", 2020 International Conference on Data Analytics for Business and Industry: Way Towards a Sustainable Economy (ICDABI), Sakheer, Bahrain (2020), <https://ieeexplore.ieee.org/document/9325629>

Maniell Workman; David Zhi Chen; Sarhan M. Musa, "Ideality Factor Based Computational Analysis of Perovskite Solar Cells", 2021 IEEE Conference on Technology for Sustainability (SusTech) (April 22-24 2021)

Maniell Workman; David Zhi Chen; Sarhan M. Musa, "Current Methods of Power Conversion Efficiency Optimization for Perovskite Solar Cells," 2021 IEEE Southeast Conference, Atlanta, GA (March 10-14 2021), <https://ieeexplore.ieee.org/document/9401870>